Energy Efficient Resource Allocation in Machine-to-Machine Communications with Multiple Access and Energy Harvesting for IoT

Zhaohui Yang, Wei Xu, *Senior Member, IEEE*, Yijin Pan, Cunhua Pan, and Ming Chen

***Abstract*—This paper studies energy efficient resource allocation for a machine-to-machine (M2M) enabled cellular network with non-linear energy harvesting, especially focusing on two different multiple access strategies, namely non-orthogonal multiple access (NOMA) and time division multiple access (TDMA). Our goal is to minimize the total energy consumption of the network via joint power control and time allocation while taking into account circuit power consumption. For both NOMA and TDMA strategies, we show that it is optimal for each machine type communication device (MTCD) to transmit with the minimum throughput, and the energy consumption of each MTCD is a convex function with respect to the allocated transmission time. Based on the derived optimal conditions for the transmission power of MTCDs, we transform the original optimization problem for NOMA to an equivalent problem which can be solved suboptimally via an iterative power control and time allocation algorithm. Through an appropriate variable transformation, we also transform the original optimization problem for TDMA to an equivalent tractable problem, which can be iteratively solved. Numerical results verify the theoretical findings and demonstrate that NOMA consumes less total energy than TDMA at low circuit power regime of MTCDs, while at high circuit power regime of MTCDs TDMA achieves better network energy efficiency than NOMA.**

***Index Terms*—Internet of Things (IoT), machine-to-machine (M2M), non-orthogonal multiple access (NOMA), energy harvesting, resource allocation.**

I. Introduction

Machine-to-machine (M2M) communications have been considered as one of the promising technologies to realize the Internet of Things (IoT) in the future 5th generation network. M2M communications can be applied to many IoT applications, which mainly involve new business models and opportunities, such as smart grids, environmental monitoring and intelligent transport systems [2]. Different from conventional human type communications, M2M communications have many unique features [3]. The unique features include massive transmissions from a large number of machine type communication devices (MTCDs), small bursty natured traffic (periodically generated), extra low power consumption of MTCDs, high requirements of energy efficiency and security.

A key challenge for M2M communications is access control, which manages the engagement of massive MTCDs to the core network. To tackle this challenge, various solutions have been proposed, e.g., by using wired access (cable, DSL) [4], wireless short distance techniques (WLAN, Bluetooth), and wide area cellular network infrastructure (Long Term Evolution-Advanced (LTE-A), WiMAX) [5]. Among all these solutions, an effective approach is to deploy machine type communication gateways (MTCGs) to act as relays of MTCDs [3]. With the help of MTCGs, all MTCDs can be successfully connected to the base station (BS) at the additional cost of energy consumption [6]–[9]. To enable multiple MTCDs to transmit data to the same MTCG, time division multiple access (TDMA) was adopted in [10]. However, since there are a vast number of MTCDs to be served, TDMA leads to large transmission delay and synchronization overhead. By splitting users in the power domain, non-orthogonal multiple access (NOMA) can simultaneously serve multiple users at the same frequency or time resource [11]. Consequently, NOMA based access scheme yields a significant gain in spectral efficiency over the conventional orthogonal TDMA [11]–[16]. This favorable characteristic makes NOMA an attractive solution for supporting massive MTCDs in M2M networks. Considering NOMA, [17] investigated an M2M enabled cellular network, where multiple MTCDs simultaneously transmit data to the same MTCG and multiple MTCGs simultaneously transmit the gathered data to the BS.

Besides, another key challenge is the energy consumption of MTCDs [18]–[20]. According to [3], the total system throughput of an M2M network is mainly limited by the energy budget of the MTCDs. To improve the system performance, energy harvesting (EH) has been applied to wireless communication networks [21]–[24]. In particular, direct and non-direct energy transfer based schemes for EH were investigated in [23], while in [24], the optimization of green-energy-powered cognitive radio networks was surveyed. Recently, the downlink resource allocation for EH in small cells was studied in [25]–[27]. By using EH, MTCDs are able to harvest wireless energy from radio frequency (RF) signals [28]–[31], and the system energy can be significantly improved. Consequently, implementing EH is promising in M2M communications especially with MTCDs configured with low power consumption. In previous

This work was supported in part by the National Nature Science Foundation of China under grants 61471114, 61372106 & 61221002, in part by the Six Talent Peaks project in Jiangsu Province under grant GDZB-005, in part by the UK Engineering and Physical Sciences Research Council under Grant EP/N029666/1, and in part by the Scientific Research Foundation of Graduate School of Southeast University under Grant YBJJ1650. This paper was presented at the IEEE Infocom Workshops 2017 in Atlanta, GA, USA [1]. (*Corresponding authors: Wei Xu; Cunhua Pan.*)

Z. Yang, W. Xu, Y. Pan, and M. Chen are with the National Mobile Communications Research Laboratory, Southeast University, Nanjing 210096, China, (Email: {yangzhaohui, wxu, panyijin, chenming}@seu.edu.cn).

C. Pan is with the School of Electronic Engineering and Computer Science, Queen Mary, University of London, London E1 4NS, U.K., (Email: c.pan@qmul.ac.uk).

wireless powered communication networks using relays [32]–[34], it was assumed that an energy constrained relay node harvests energy from RF signals and the relay uses that harvested energy to forward source information to destination. Due to the extra low power budget of MTCDs in M2M communications, it is reasonable to let the MTCD transmit data to an MTCG, and then the MTCG relays the information while the MTCD simultaneously harvests energy from the MTCG, which is different from existing works, e.g., [32]–[34]. Enabling the source node to harvest energy from the relay node, a power-allocation scheme for a decode-and-forward relaying-enhanced wireless system was proposed in [35] with one source node, one relay node and one destination node.

The above-mentioned energy consumption models, considered in [1], [8]–[10], [17]–[19], [28]–[31], are only concerned with the RF transmission power and ignore the circuit power consumption of MTCDs and MTCGs. However, as stated in [36], the circuit power consumption is non-negligible compared to RF transmission power. Without considering the circuit power consumption, energy saving can always benefit from longer transmission time [37], [38]. While considering the circuit power consumption which definitely exists in practice, the results vary significantly in that it can not be always energy efficient for long transmission time due to the fact that the total energy consumption becomes infinity as transmission time goes infinity. Hence, it is of importance to investigate the optimal transmission time when taking into account the circuit power consumption in applications.

Given access control and energy consumption challenges in M2M communications, both TDMA and NOMA based M2M networks with EH are proposed in this work. The MTCDs first transmit data to the corresponding MTCGs, and then MTCGs transmit wireless information to the BS and wireless energy to the MTCDs. To prolong the lifetime of the considered network, the harvested energy for each MTCD is set to be no less than the consumed energy in information transmission (IT) stage. The main contributions of this paper are summarized as follows:

- We formulate the total energy minimization problem for the M2M enabled cellular network with non-linear energy harvesting (EH) model via joint power control and time allocation. In the non-linear EH model, we consider the receiver sensitivity, on which energy conversion starts beyond a threshold. Besides, we explicitly take into account the circuit energy consumption of both MTCDs and MTCGs. All theses factors are critical in practical applications which inevitably affect the system performance. Specifically, the non-linear EH model leads to a non-smooth objective function and non-smooth constraints, and the circuit energy consumption affects the optimal transmission time of the system.
- For the NOMA strategy, we observe that: 1) it is optimal for each MTCD to transmit with minimal throughput; 2) it is further revealed that the energy consumption of each MTCD is a convex function with respect to the allocated transmission time. Given these observations, it indicates that a globally optimal transmission time always exists that the optimal transmission time equals the maximally allowed transmission time if it does not exceed a quantified threshold derived in closed form.
- To solve the original total energy minimization problem for the NOMA strategy, we devise a low-complexity iterative power control and time allocation algorithm. Specifically, to deal with the non-smooth EH function, we introduce new sets during which MTCDs can effectively harvest energy. Given new sets, the EH function of MTCDs can be presented as a continuous one. Moreover, to deal with nonconvex objective function, nonconvex minimal throughput constraints, and nonconvex energy causality constraints, we transform these nonconvex ones into convex ones by manipulations with the optimal conditions. The convergence of the iterative algorithm is strictly proved.
- For the TDMA strategy, we verify that the two observations for NOMA are also valid. Although the original total energy minimization problem for the TDMA strategy is nonconvex, the problem can be transformed into an equivalent tractable one, which can be iteratively solved to its suboptimality. For the total energy minimization, numerical results identify that NOMA is superior over TDMA at small circuit power regime of MTCDs, while TDMA outperforms NOMA at large circuit power regime of MTCDs.

This paper is organized as follows. In Section II, we introduce the system and power consumption model. Section III and Section IV provide the energy efficient resource allocation for NOMA and TDMA, respectively. Numerical results are displayed in Section V and conclusions are drawn in Section VI.

II. System and Power Consumption Model

A. System Model

Consider an uplink M2M enabled cellular network with N MTCGs and M MTCDs, as shown in Fig. 1. Denote the sets of MTCGs and MTCDs by $\mathcal{N} = \{1, \cdots, N\}$ and $\mathcal{M} = \{1, \cdots, M\}$, respectively. Each MTCG serves as a relay for some MTCDs. Assume that the decode-and-forward protocol [39] is adopted at each MTCG. Denote $\mathcal{J}_i = \{J_{i-1}+1, \cdots, J_i\}$ as the specific set of MTCDs served by MTCG $i \in \mathcal{N}$, where $J_0 = 0$, $J_N = M$, $J_i = \sum_{l=1}^{i} |\mathcal{J}_l|$, and $|\cdot|$ is the cardinality of a set.[1] To reduce the receiver complexity at the MTCG, the maximal number of MTCDs associated to one MTCG is set as four. Obviously, we have $\bigcup_{i\in\mathcal{N}} \mathcal{J}_i = \mathcal{M}$.

B. NOMA Strategy

In time constraint T, each MTCD has some payloads to transmit to the BS. By using superposition coding at the transmitter and successive interference cancellation (SIC) at

[1]In this paper, we assume that MTCDs are already associated to MTCGs by using the cluster formation methods for M2M communications, e.g., in [40]–[43]. Joint optimization of cluster formation and resource allocation in M2M communications with NOMA/TDMA and EH can certainly further improve the performance, but we leave it in future work in order to focus on the power control and time allocation in the current submission.

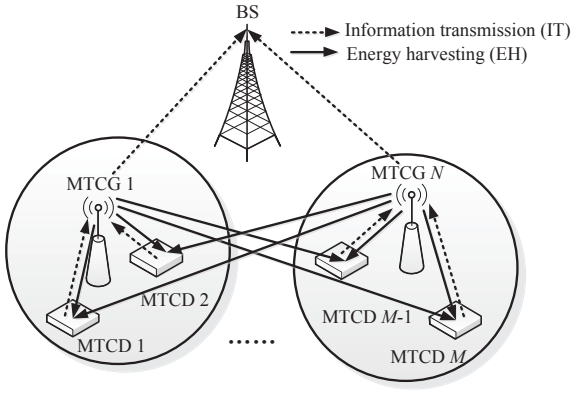

Fig. 1. The considered uplink M2M enabled cellular network.

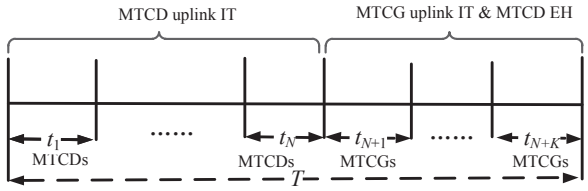

Fig. 2. Time sharing scheme for NOMA strategy during one uplink transmission period.

the receiver, multiple MTCDs (or MTCGs) can simultaneously transmit signals to the corresponding receiver using NOMA. To reduce the receiver complexity and error propagation due to SIC, it is reasonable for the same resource to be multiplexed by a small number (usually two to four) of devices [44]. Considering the receiver complexity at the BS, the sets of MTCGs are further classified into multiple small clusters. For MTCGs, the set $\mathcal{N}$ is classified into K clusters. Let $\mathcal{K} = \{1, 2, \cdots, K\}$ be the set of clusters. Denote $\mathcal{I}_k = \{I_{k-1} + 1, \cdots, I_k\}$ as the specific set of MTCGs in cluster $k \in \mathcal{K}$, where $I_0 = 0$, $I_K = N$, $I_k = \sum_{l=1}^{k} |\mathcal{I}_l|$, and $|\mathcal{I}_k| \leq 4$.[2]

Note that our major motivation of using NOMA is to enhance the ability of serving more terminals simultaneously [11]. However, the number of terminals occupying the same resource cannot be arbitrarily large in order to make NOMA effective in practice. Therefore, if there would be an even higher number of IoT terminals, we believe that a number of ways including NOMA should be further incorporated to better address the access problem for higher number of IoT terminals [47].

As depicted in Fig. 2, time T consists of $N + K$ uplink transmission phases for MTCDs and MTCGs. NOMA is adopted for MTCDs to transmit data to MTCGs in the first N phases. Both NOMA and EH are in operation in the last K phases where MTCGs transmit data to the BS and simultaneously MTCDs harvest energy from all MTCGs. In the i-th ($i \leq N$) phase with allocated time t_i, all MTCDs in $\mathcal{J}_i$ simultaneously transmit data to MTCG i according to the NOMA principle and MTCG i detects the signal. In the $(N + k)$-th ($k \leq K$) phase with allocated time t_{N+k}, all MTCGs in $\mathcal{I}_k$ simultaneously transmit the decoded data from the served MTCDs to the BS by using the NOMA strategy. As a result, we have the following transmission time constraint

$$\sum_{i=1}^{N+K} t_i \leq T. \tag{1}$$

In the i-th ($i \leq N$) phase, all MTCDs in $\mathcal{J}_i$ simultaneously transmit data to MTCG i following the NOMA principle. The received signal of MTCG i is

$$y_i = \sum_{j=J_{i-1}+1}^{J_i} h_{ij}\sqrt{p_j}s_j + n_i, \tag{2}$$

where h_{ij} is the channel between MTCD j and MTCG i, p_j denotes the transmission power of MTCD j, s_j is the transmitted message of MTCD j, and n_i represents the additive zero-mean Gaussian noise with variance σ^2. Without loss of generality, the channels are sorted as $|h_{i(J_{i-1}+1)}|^2 \geq \cdots \geq |h_{iJ_i}|^2$. By applying SIC to decode the signals [14]–[16], the achievable throughput of MTCD $j \in \mathcal{J}_i$ is

$$r_{ij} = Bt_i \log_2 \left(1 + \frac{|h_{ij}|^2 p_j}{\sum_{l=j+1}^{J_i} |h_{il}|^2 p_l + \sigma^2}\right), \tag{3}$$

where B is the available bandwidth for transmission. Note that we consider the case where MTCDs associated to different MTCGs are allocated with orthogonal time resource. Therefore, the interference from other MTCDs associated to different MTCDs is ignored.

In the $(N+k)$-th ($k \leq K$) phase with allocated time t_{N+k}, after having successfully decoded the messages in the last N phases, MTCGs in $\mathcal{I}_k$ simultaneously transmit the gathered data to the BS based on the NOMA principle. Denote the channel between MTCG i and the BS by h_i. Without loss of generality, the channels are sorted as $|h_{I_{k-1}+1}|^2 \geq \cdots \geq |h_{I_k}|^2$, $\forall k \in \mathcal{K}$. Hence, the achievable throughput of MTCG $i \in \mathcal{I}_k$ can be expressed as [14]–[16]

$$r_i = Bt_{N+i} \log_2 \left(1 + \frac{|h_i|^2 q_i}{\sum_{n=i+1}^{I_k} |h_n|^2 q_n + \sigma^2}\right), \tag{4}$$

where q_i is the transmission power of MTCG i.

According to [3], MTCDs are always equipped with finite batteries, which limit the lifetime of the M2M enabled cellular network. To further prolong the lifetime, EH technology is adopted for MTCDs to harvest energy remotely from RF signals radiated by MTCGs [22]. Specifically, each MTCD harvests energy when MTCGs transmit data to the BS. Since the noise power is much smaller than the received power of MTCGs in practice [48]–[50], the energy harvested from the channel noise is negligible. Assume that uplink channel and downlink channel follow the channel reciprocity [51]. The

[2]A scheme for cluster formation for uplink NOMA is in [45]. According to [45] and [46], one common scheme with two devices in each cluster is the strong-weak scheme, i.e., the device with the strongest channel condition is paired with the device with the weakest, and the device with the second strongest is paired with one with the second weakest, and so on.

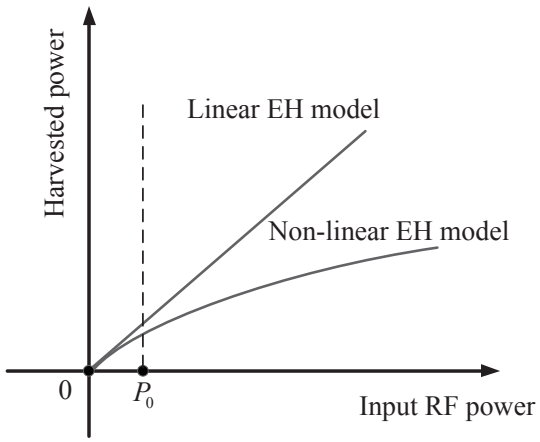

Fig. 3. Comparison between the linear and non-linear EH model.

total energy harvested by MTCD j served by MTCG i can be evaluated as

$$E_{ij}^{\mathrm{H}} = \sum_{k=1}^{K} t_{N+k} u \left(\sum_{n=I_{k-1}+1}^{I_k} |h_{nj}|^2 q_n \right), \quad \forall i \in \mathcal{N}, j \in \mathcal{J}_i, \tag{5}$$

where $\sum_{n=I_{k-1}+1}^{I_k} |h_{nj}|^2 q_n$ is the received RF power of MTCD j during time t_{N+k}, and function $u(\cdot)$ captures the EH model which maps input RF power into harvested power. Two commonly used EH models are shown in Fig. 3, i.e., linear and non-linear EH models. According to [52] and [53], linear EH model may lead to resource allocation mismatch. In order to capture the effects of practical EH circuits on the end-to-end power conversion, we adopt the more practical non-linear EH model proposed in [52]:

$$u(x) = \begin{cases} \frac{M(1+\mathrm{e}^{ab})}{\mathrm{e}^{ab}+\mathrm{e}^{-a(x-2b)}} - \frac{M}{\mathrm{e}^{ab}}, & \text{if } x \geq P_0 \\ 0, & \text{elsewise} \end{cases}, \tag{6}$$

where a, b, M and P_0 are positive parameters which capture the joint effects of different non-linear phenomena caused by hardware constraints. Note that P_0 is the receiver sensitivity threshold of each MTCD, in which energy conversion starts. Hence, it is possible that some MTCDs cannot effectively harvest energy in some slots, since the received power is below the receiver sensitivity threshold P_0.

The total energy consumption of the M2M enabled communication network consists of two parts: the energy consumed by MTCDs and MTCGs. For each part, the energy consumption of a transmitter consists of both RF transmission power and circuit power due to hardware processing [54]. According to [55], the energy consumption when MTCDs or MTCGs are in idle model, i.e., do not transmit RF signals, is negligible.

During the i-th ($i \leq N$) phase, MTCD $j \in \mathcal{J}_i$ served by MTCG i just transmits data to MTCG i with allocated time t_i and transmission power p_j. Thus, the energy E_{ij} consumed by MTCD $j \in \mathcal{J}_i$ can be modeled as

$$E_{ij} = t_i \left(\frac{p_j}{\eta} + P^{\mathrm{C}} \right), \quad \forall i \in \mathcal{N}, j \in \mathcal{J}_i, \tag{7}$$

where $\eta \in (0, 1]$ and P^{C} denote the power amplifier (PA) efficiency and the circuit power consumption of each MTCD, respectively. According to the energy causality constraint in EH networks, E_{ij} has to satisfy $E_{ij} \leq E_{ij}^{\mathrm{H}}$. Summing the energy consumed by all MTCDs in $\mathcal{J}_i$, we can obtain the energy E_i consumed during the i-th phase as

$$E_i = \sum_{j=J_{i-1}+1}^{J_i} E_{ij}, \quad \forall i \in \mathcal{N}. \tag{8}$$

During the $(N+k)$-th phase, the system energy consumption, denoted by E_{N+k}, is modeled as

$$E_{N+k} = \sum_{i=I_{k-1}+1}^{I_k} t_{N+k} \left(\frac{q_i}{\xi} + Q^{\mathrm{C}} \right) - \sum_{i=1}^{N} \sum_{j=J_{i-1}+1}^{J_i} t_{N+k} u \left(\sum_{n=I_{k-1}+1}^{I_k} |h_{nj}|^2 q_n \right), \tag{9}$$

where $\xi \in (0, 1]$ and Q^{C} are the PA efficiency and the circuit power consumption of each MTCG, respectively. According to the law of energy conservation [56], we must have

$$\sum_{i=I_{k-1}+1}^{I_k} t_{N+k} q_i - \sum_{i=1}^{N} \sum_{j=J_{i-1}+1}^{J_i} t_{N+k} u \left(\sum_{n=I_{k-1}+1}^{I_k} |h_{nj}|^2 q_n \right) > 0, \tag{10}$$

which is the energy loss due to wireless propagation.

Based on (5)-(9), the total energy consumption, E_{Tot}, of the whole system during time T can be expressed as

$$\begin{aligned} E_{\mathrm{Tot}} &= \sum_{i=1}^{N+K} E_i \\ &= \sum_{i=1}^{N} \sum_{j=J_{i-1}+1}^{J_i} t_i \left(\frac{p_j}{\eta} + P^{\mathrm{C}} \right) \\ &\quad + \sum_{k=1}^{K} \sum_{i=I_{k-1}+1}^{I_k} t_{N+k} \left(\frac{q_i}{\xi} + Q^{\mathrm{C}} \right) \\ &\quad - \sum_{k=1}^{K} \sum_{i=1}^{N} \sum_{j=J_{i-1}+1}^{J_i} t_{N+k} u \left(\sum_{n=I_{k-1}+1}^{I_k} |h_{nj}|^2 q_n \right). \end{aligned} \tag{11}$$

C. TDMA Strategy

With the TDMA strategy, time T consists of $M+N$ uplink transmission phases for MTCDs and MTCGs, as illustrated in Fig. 4. All MTCDs transmit data to the corresponding MTCGs in the first M phases with TDMA, and all MTCGs transmit the collected data to the BS in the last N phases with TDMA. Then, we obtain the following transmission time constraint

$$\sum_{i=1}^{M+N} t_i \leq T. \tag{12}$$

In the j-th ($j \leq M$) phase, MTCD $j \in \mathcal{J}_i$ transmits data to its serving MTCG i with achievable throughput

$$r_{ij} = B t_j \log_2 \left(1 + \frac{|h_{ij}|^2 p_j}{\sigma^2} \right), \quad \forall i \in \mathcal{N}, j \in \mathcal{J}_i. \tag{13}$$

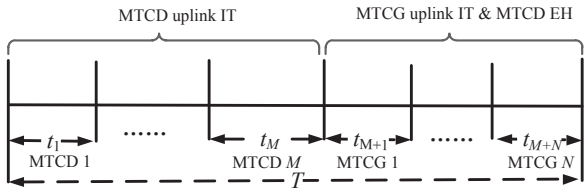

Fig. 4. Time sharing scheme for TDMA strategy during one uplink transmission period.

In the $(M+i)$-th phase, after having decoded all the messages of its served MTCDs, MTCG i transmits the collected data to the BS with achievable throughput

$$r_i = Bt_{M+i}\log_2\left(1+\frac{|h_i|^2 q_i}{\sigma^2}\right), \quad \forall i \in \mathcal{N}. \tag{14}$$

Similar to (5), the total energy harvested of MTCD j served by MTCG i is

$$E_{ij}^{\mathrm{H}} = \sum_{n=1}^{N} t_{M+n} u(|h_{nj}|^2 q_n), \quad \forall i \in \mathcal{N}, j \in \mathcal{J}_i. \tag{15}$$

According to (6), it is possible that some MTCDs cannot effectively harvest energy in some slots, due to the fact that the received power is below the receiver sensitivity threshold P_0.

As in (7) and (9), the energy consumption of a transmitter includes both RF transmission power and circuit power [54]. With allocated transmission time t_j, the energy E_{ij} consumed by MTCD $j \in \mathcal{J}_i$ can be modeled as

$$E_{ij} = t_j\left(\frac{p_j}{\eta} + P^{\mathrm{C}}\right), \quad \forall i \in \mathcal{N}, j \in \mathcal{J}_i. \tag{16}$$

With allocated transmission time t_{M+i}, the system energy consumption, denoted by E_{M+i}, is modeled as

$$E_{M+i} = t_{M+i}\left(\frac{q_i}{\xi} + Q^{\mathrm{C}}\right) - \sum_{n=1}^{N}\sum_{j=J_{n-1}+1}^{J_n} t_{M+i} u(|h_{ij}|^2 q_i), \tag{17}$$

where $\sum_{n=1}^{N}\sum_{j=J_{n-1}+1}^{J_n} t_{M+i} u(q_i|h_{ij}|^2)$ is the energy harvested by all MTCDs during the transmission time t_{M+i} for MTCG i to transmit data to the BS.

According to (15)-(17), the total energy consumption, E_{Tot}, of the whole system during time T can be expressed as

$$\begin{aligned} E_{\mathrm{Tot}} &= \sum_{i=1}^{N}\sum_{j=J_{i-1}+1}^{J_i} E_{ij} + \sum_{i=M+1}^{M+N} E_i \\ &= \sum_{i=1}^{N}\sum_{j=J_{i-1}+1}^{J_i} t_j\left(\frac{p_j}{\eta}+P^{\mathrm{C}}\right) + \sum_{i=1}^{N} t_{M+i}\left(\frac{q_i}{\xi}+Q^{\mathrm{C}}\right) \\ &\quad - \sum_{i=1}^{N}\sum_{j=J_{i-1}+1}^{J_i}\sum_{n=1}^{N} t_{M+n} u(|h_{nj}|^2 q_n). \end{aligned} \tag{18}$$

III. Energy Efficient Resource Allocation for NOMA

In this section, we study the resource allocation for an uplink M2M enabled cellular network with NOMA and EH. Specifically, we aim at minimizing the total energy consumption via jointly optimizing power control and time allocation for NOMA. The system energy minimization problem is formulated as

$$\min_{\boldsymbol{p},\boldsymbol{q},\boldsymbol{t}} \ E_{\mathrm{Tot}} \tag{19a}$$

$$\text{s.t.} \ \ r_{ij} \geq D_j, \quad \forall i \in \mathcal{N}, j \in \mathcal{J}_i \tag{19b}$$

$$r_i \geq \sum_{j=J_{i-1}+1}^{J_i} D_j, \quad \forall i \in \mathcal{N} \tag{19c}$$

$$E_{ij} \leq E_{ij}^{\mathrm{H}}, \quad \forall i \in \mathcal{N}, j \in \mathcal{J}_i \tag{19d}$$

$$\sum_{i=1}^{N+K} t_i \leq T \tag{19e}$$

$$0 \leq p_j \leq P_j, 0 \leq q_i \leq Q_i, \quad \forall i \in \mathcal{N}, j \in \mathcal{J}_i \tag{19f}$$

$$\boldsymbol{t} \geq \mathbf{0}, \tag{19g}$$

where $\boldsymbol{p} = [p_1, \cdots, p_M]^T$, $\boldsymbol{q} = [q_1, \cdots, q_N]^T$, $\boldsymbol{t} = [t_1, \cdots, t_{N+K}]^T$, D_j is the payload that MTCD j has to upload within time constraint T, P_j is the maximal transmission power of MTCD j, and Q_i is the maximal transmission power of MTCG i. It is assumed that all payloads are positive, i.e., $D_j > 0$, for all j. The objective function (19a) defined in (11) is the total energy consumption of both MTCDs and MTCGs. Constraints (19b) and (19c) reflect that the minimal required payloads for MTCDs can be uploaded to the BS. The consumed energy of each MTCD should not exceed its harvested energy in time T, as stated in (19d). Constraints (19e) reflect that the payloads for all MTCDs are transmitted in time T.

Note that problem (19) is nonconvex due to nonconvex objective function (19a) and constraints (19b)-(19d). In general, there is no standard algorithm for solving nonconvex optimization problems. In the following, we first find the optimal conditions for problem (19) by exploiting the special structure of the uplink NOMA rate, and then provide an iterative power control and time allocation algorithm.

A. Optimal Conditions

By analyzing problem (19), we have the following lemma.

Lemma 1: The optimal solution $(\boldsymbol{p}^*, \boldsymbol{q}^*, \boldsymbol{t}^*)$ to problem (19) satisfies

$$r_{ij}^* = D_j, \quad \forall i \in \mathcal{N}, j \in \mathcal{J}_i. \tag{20}$$

This observation states that the minimal throughput leads to more energy saving, which is similar to [17] and is also widely known in the information theory community.

Lemma 1 states that the optimal transmit throughput for each MTCD is required minimum. Note that the optimal throughput for each MTCG is not always as its minimum requirement, i.e., constraints (19c) are active at the optimum, since MTCGs should transmit more power to maintain that the harvested energy of each MTCD is no less than the consumed energy.

Based on Lemma 1, we further have the following lemma about the optimal transmission power of MTCDs.

Lemma 2: If $(\boldsymbol{p}^*, \boldsymbol{q}^*, \boldsymbol{t}^*)$ is the optimal solution to problem (19), we have

$$p_j^* = \sum_{l=j+1}^{J_i} \frac{\sigma^2}{|h_{ij}|^2}\left(\mathrm{e}^{\frac{a_l}{t_i^*}}-1\right)\left(\mathrm{e}^{\frac{a_j}{t_i^*}}-1\right)\mathrm{e}^{\frac{b_{jl}}{t_i^*}} + \frac{\sigma^2}{|h_{ij}|^2}\left(\mathrm{e}^{\frac{a_j}{t_i^*}}-1\right), \quad \forall i \in \mathcal{N}, j \in \mathcal{J}_i, \tag{21}$$

where

$$a_l = \frac{(\ln 2) D_l}{B}, \quad b_{jl} = \frac{\sum_{s=j+1}^{l-1} (\ln 2) D_s}{B}, \quad \forall i \in \mathcal{N}, j, l \in \mathcal{J}_i. \tag{22}$$

Besides, the optimal transmission power p_j^* of MTCD $j \in \mathcal{J}_i$ is always non-negative and decreases with the transmission time t_i^*.

Please refer to Appendix A.

From Lemma 2, large transmission time results in low transmission power. This is reasonable as the minimal payload is limited and large transmission time requires low achievable rate measured in bits/s. It is also revealed from Lemma 2 that the optimal transmission power of MTCD $j \in \mathcal{J}_i$ served by MTCG i depends only on the variable of the allocated transmission time t_i. As a result, the energy E_{ij} consumed by MTCD j in $\mathcal{J}_i$ is a function of the allocated transmission time t_i. Based on (7) and (21), we have

$$E_{ij} = \sum_{l=j+1}^{J_i} \frac{\sigma^2 t_i}{\eta |h_{ij}|^2}\left(\mathrm{e}^{\frac{a_l}{t_i}}-1\right)\left(\mathrm{e}^{\frac{a_j}{t_i}}-1\right)\mathrm{e}^{\frac{b_{jl}}{t_i}} + \frac{\sigma^2 t_i}{\eta |h_{ij}|^2}\left(\mathrm{e}^{\frac{a_j}{t_i}}-1\right) + t_i P_{\mathrm{C}}. \tag{23}$$

Theorem 1: The energy E_{ij} defined in (23) is convex with respect to (w.r.t.) the transmission time t_i. When $P^{\mathrm{C}} = 0$, the energy E_{ij} monotonically decreases with t_i. When $P^{\mathrm{C}} > 0$, the energy E_{ij} first decreases with t_i when $0 \le t_i \le T_{ij}^*$ and then increases with t_i when $t_i > T_{ij}^*$, where T_{ij}^* is the unique zero point of the first-order derivative $\frac{\partial E_{ij}}{\partial t_i}$, i.e.,

$$\left.\frac{\partial E_{ij}}{\partial t_i}\right|_{t_i = T_{ij}^*} = 0. \tag{24}$$

Please refer to Appendix B.

Fig. 5 exemplifies the energy E_{ij} given in (23) versus t_i. When $P^{\mathrm{C}} = 0$, i.e., the circuit energy consumption of MTCDs is not considered, we come to the same conclusion as in [37] and [38] that the consumed energy decreases as the transmission time increases according to Theorem 1. Without considering the circuit power consumption, $R = \log_2(1+\mathrm{SNR})$ and the energy efficiency increases with the decrease of power. Consequently, when $P^{\mathrm{C}} = 0$ and the minimal throughput demand D_j is given, the consumed energy E_{ij} is a decreasing function w.r.t. t_i. This fundamentally follows the Shannon's law.

When $P^{\mathrm{C}} > 0$, i.e., the circuit energy consumption of MTCDs is taken into account, however, we find from Theorem 1 that the consumed energy first decreases and then increases with the transmission time, which is different from the previous conclusion in [37] and [38]. This is because that the total energy contains two parts balancing each other, i.e., the RF transmission energy part which monotonically decreases with the transmission time and the circuit energy part which linearly increases with the transmission time. In the following of this section, we assume that the circuit power consumption of MTCDs and MTCGs is in general positive, i.e., $P^{\mathrm{C}} > 0$ and $Q^{\mathrm{C}} > 0$.

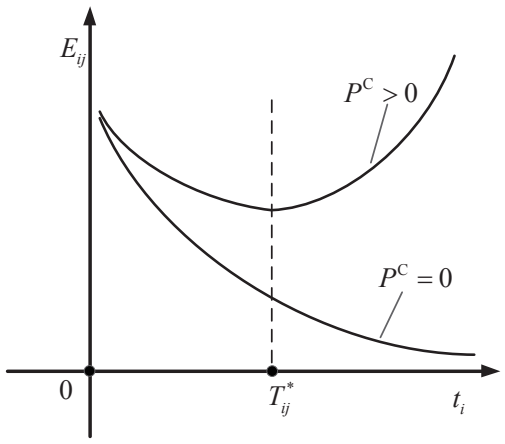

Fig. 5. The energy E_{ij} versus transmission time t_i.

Theorem 2: If $T \le \max_{\forall i \in \mathcal{N}} \min_{\forall j \in \mathcal{J}_i} \{T_{ij}^*\}$, the optimal time allocation $\boldsymbol{t}^*$ to problem (19) satisfies

$$\sum_{i=1}^{N+K} t_i^* = T. \tag{25}$$

If $T \ge T_{\mathrm{Upp}}$, where T_{Upp} is defined in (C.4), the optimal time allocation $\boldsymbol{t}^*$ to problem (19) satisfies

$$\sum_{i=1}^{N+K} t_i^* < T. \tag{26}$$

Please refer to Appendix C.

From Theorem 2, it is observed that transmitting with the maximal transmission time T is optimal when T is not large. This is because that the reduced energy of RF transmission dominates the additional energy of circuit by increasing transmission time. When the available time T becomes large enough, Theorem 2 states that it is not optimal to transmit with the maximal transmission time T. This is due to the fact that the increased energy of circuit power dominates the power consumption while the energy reduction of RF transmission becomes relatively marginal.

B. Joint Power Control and Time Allocation Algorithm

Problem (19) has two difficulties: one comes from the non-smooth EH function defined in (6), and the other one is the non-convexity of both objective function (19a) and constraints (19b)-(19d). To deal with the first difficulty, we introduce notation $\mathcal{S}_{ij}$ as the set of phases during which

MTCD $j \in \mathcal{J}_i$ can effectively harvest energy, i.e., $\mathcal{S}_{ij} = \{k| \sum_{n=I_{k-1}+1}^{I_k} |h_{nj}|^2 q_n > P_0, \forall k \in \mathcal{K}\}$. With $\mathcal{S}_{ij}$ in hand, the harvested power of MTCD $j \in \mathcal{J}_i$ can be presented by the smooth function $\bar{u}(x)$ defined in (28). To deal with the second difficulty, we substitute (3)-(7), (11) and (21) into (19), and the original problem (19) with fixed sets $\mathcal{S}_{ij}$'s can be equivalently transformed into the following problem:

$$\begin{aligned}\min_{\boldsymbol{q},\boldsymbol{t}} \ & \sum_{i=1}^{N}\sum_{j=J_{i-1}+1}^{J_i}\sum_{l=j+1}^{J_i}\frac{\sigma^2 t_i}{\eta|h_{ij}|^2}\left(\mathrm{e}^{\frac{a_l}{t_i}}-1\right)\left(\mathrm{e}^{\frac{a_j}{t_i}}-1\right)\mathrm{e}^{\frac{b_{jl}}{t_i}} \\ & +\sum_{i=1}^{N}\sum_{j=J_{i-1}+1}^{J_i}\frac{\sigma^2 t_i}{\eta|h_{ij}|^2}\left(\mathrm{e}^{\frac{a_j}{t_i}}-1\right)+\sum_{i=1}^{N}\sum_{j=J_{i-1}+1}^{J_i} t_i P^{\mathrm{C}} \\ & +\sum_{k=1}^{K}\sum_{i=I_{k-1}+1}^{I_k} t_{N+k}\left(\frac{q_i}{\xi}+Q^{\mathrm{C}}\right) \\ & -\sum_{i=1}^{N}\sum_{j=J_{i-1}+1}^{J_i}\sum_{k\in\mathcal{S}_{ij}} t_{N+k}\bar{u}\left(\sum_{n=I_{k-1}+1}^{I_k}|h_{nj}|^2 q_n\right) \quad (27a)\end{aligned}$$

$$\text{s.t. } |h_i|^2 q_i \geq \left(2^{\frac{\sum_{j\in\mathcal{J}_i} D_j}{B t_{N+1}}}-1\right)\left(\sum_{l=i+1}^{I_k}|h_l|^2 q_l+\sigma^2\right), \quad \forall k \in \mathcal{K}, i \in \mathcal{I}_k \quad (27b)$$

$$\begin{aligned}& \sum_{l=j+1}^{J_i}\frac{\sigma^2}{\eta|h_{ij}|^2} t_i\left(\mathrm{e}^{\frac{a_l}{t_i}}-1\right)\left(\mathrm{e}^{\frac{a_j}{t_i}}-1\right)\mathrm{e}^{\frac{b_{jl}}{t_i}} \\ & +\frac{\sigma^2}{\eta|h_{ij}|^2} t_i\left(\mathrm{e}^{\frac{a_j}{t_i}}-1\right)+t_i P^{\mathrm{C}} \\ & \leq \sum_{k\in\mathcal{S}_{ij}} t_{N+k}\bar{u}\left(\sum_{n=I_{k-1}+1}^{I_k}|h_{nj}|^2 q_n\right), \quad \forall i \in \mathcal{N}, j \in \mathcal{J}_i \quad (27c)\end{aligned}$$

$$\sum_{n=I_{k-1}+1}^{I_k}|h_{nj}|^2 q_n \geq P_0, \ \ \forall i \in \mathcal{N}, j \in \mathcal{J}_i, k \in \mathcal{S}_{ij} \quad (27d)$$

$$\sum_{i=1}^{N+K} t_i \leq T \quad (27e)$$

$$\begin{aligned}& \sum_{l=j+1}^{J_i}\frac{\sigma^2}{|h_{ij}|^2}\left(\mathrm{e}^{\frac{a_l}{t_i}}-1\right)\left(\mathrm{e}^{\frac{a_j}{t_i}}-1\right)\mathrm{e}^{\frac{b_{jl}}{t_i}} \\ & +\frac{\sigma^2}{|h_{ij}|^2}\left(\mathrm{e}^{\frac{a_j}{t_i}}-1\right) \leq P_j, \quad \forall i \in \mathcal{N}, j \in \mathcal{J}_i \quad (27f)\end{aligned}$$

$$0 \leq q_i \leq Q_i, \quad \forall i \in \mathcal{N} \quad (27g)$$

$$\boldsymbol{t} \geq \mathbf{0}, \quad (27h)$$

where

$$\bar{u}(x) = \frac{M(1+\mathrm{e}^{ab})}{\mathrm{e}^{ab}+\mathrm{e}^{-a(x-2b)}} - \frac{M}{\mathrm{e}^{ab}}, \quad \forall x \geq 0. \quad (28)$$

Problem (27) is still nonconvex w.r.t. $(\boldsymbol{q}, \boldsymbol{t})$ due to nonconvex objective function (27a) and constraints (27b)-(27c). Before solving problem (27), we have the following theorem.

Theorem 3: Given transmission time $\boldsymbol{\tau} = [t_{N+1}, \cdots, t_{N+K}]^T$, problem (27) is a convex problem w.r.t. $(\boldsymbol{q}, \bar{\boldsymbol{t}})$, where $\bar{\boldsymbol{t}} = [t_1, \cdots, t_N]^T$. Given $(\boldsymbol{q}, \bar{\boldsymbol{t}})$, problem (27) is equivalent to a linear problem w.r.t. $\boldsymbol{\tau}$.

Please refer to appendix D.

According to Theorem 3, problem (27) with given transmission time $\boldsymbol{\tau}$ can be effectively solved by using the standard convex optimization method, such as interior point method [57]. Besides, problem (27) with given $(\boldsymbol{q}, \bar{\boldsymbol{t}})$ is a linear problem, which can be optimally solved via the simplex method. Based on Theorem 3, we propose an iterative power control and time allocation for NOMA (IPCTA-NOMA) algorithm with low complexity to obtain a suboptimal solution of problem (19). The idea is to iteratively update sets $\mathcal{S}_{ij}$'s according to the power and time variables obtained in the previous step.

Algorithm 1: Iterative Power Control and Time Allocation for NOMA (IPCTA-NOMA) Algorithm

1: Set $\mathcal{S}_{ij}^{(0)} = \{k | j \in \cup_{n\in\mathcal{I}_k}\mathcal{J}_n, k \in \mathcal{K}\}$, $\forall i \in \mathcal{I}$, $j \in \mathcal{J}_{ij}$, initialize a feasible solution $(\boldsymbol{q}^{(0)}, \boldsymbol{t}^{(0)})$ to problem (27) with $\mathcal{S}_{ij}^{(0)}$'s, the tolerance θ, the iteration number $v = 0$, and the maximal iteration number $V_{\max}$.
2: **repeat**
3: Set $\boldsymbol{\tau}^* = [t_{N+1}^{(v)}, \cdots, t_{N+K}^{(v)}]^T$.
4: **repeat**
5: Obtain the optimal $(\boldsymbol{q}^*, \bar{\boldsymbol{t}}^*)$ of convex problem (27) with fixed $\boldsymbol{\tau}^*$ and sets $\mathcal{S}_{ij}^{(v)}$.
6: Obtain the optimal $\boldsymbol{\tau}^*$ of linear problem (27) with fixed $(\boldsymbol{q}^*, \bar{\boldsymbol{t}}^*)$ and sets $\mathcal{S}_{ij}^{(v)}$.
7: **until** the objective value (27a) with fixed sets $\mathcal{S}_{ij}^{(v)}$ converges.
8: Set $v = v + 1$.
9: Denote $\boldsymbol{q}^{(v)} = \boldsymbol{q}^*$, $\boldsymbol{t}^{(v)} = [\bar{\boldsymbol{t}}^{*T}, \boldsymbol{\tau}^{*T}]^T$.
10: Calculate the objective value (27a) with fixed sets $\mathcal{S}_{ij}^{(v)}$ as $U_{\text{Obj}}^{(v)} = E_{\text{Tot}}(\boldsymbol{q}^{(v)}, \boldsymbol{t}^{(v)})$.
11: Update $\mathcal{S}_{ij}^{(v)} = \{k| \sum_{n=I_{k-1}+1}^{I_k} |h_{nj}|^2 q_n^{(v)} > P_0, \forall k \in \mathcal{K}\}$, $\forall i \in \mathcal{I}, j \in \mathcal{J}_i$.
12: **until** $v \geq 1$ and $|U_{\text{Obj}}^{(v)} - U_{\text{Obj}}^{(v-1)}|/U_{\text{Obj}}^{(v-1)} < \theta$ or $v > V_{\max}$.

C. Convergence and Complexity Analysis

Theorem 4: Assuming $V_{\max} \to \infty$, the sequence $(\boldsymbol{q}, \boldsymbol{t})$ generated by the IPCTA-NOMA algorithm converges.

Please refer to Appendix E.

According to the IPCTA-NOMA algorithm, the major complexity lies in solving the convex problem (27) with fixed $\boldsymbol{\tau}$. Considering that the dimension of the variables in problem (27) with fixed $\boldsymbol{\tau}$ is $2N$, the complexity of solving problem (27) with fixed $\boldsymbol{\tau}$ by using the standard interior point method is $\mathcal{O}(N^3)$ [57, Pages 487, 569]. As a result, the total complexity of the proposed IPCTA-NOMA algorithm is $\mathcal{O}(L_{\text{NO}} L_{\text{IT}} N^3)$, where L_{NO} denotes the number of outer iterations of the IPCTA-NOMA algorithm, and L_{IT} denotes the number of inner iterations of the IPCTA-NOMA algorithm for iteratively solving nonconvex problem (27) with fixed sets $\mathcal{S}_{ij}$'s.

IV. Energy Efficient Resource Allocation for TDMA

In this section, we study the energy minimization for the M2M enabled cellular network with TDMA. According to (13)-(16) and (18), the energy minimization problem can be formulated as

$$\min_{\boldsymbol{p},\boldsymbol{q},\hat{\boldsymbol{t}}} \sum_{i=1}^{N}\sum_{j=J_{i-1}+1}^{J_i} t_j\left(\frac{p_j}{\eta}+P^{\mathrm{C}}\right)+\sum_{i=1}^{N} t_{M+i}\left(\frac{q_i}{\xi}+Q^{\mathrm{C}}\right) - \sum_{i=1}^{N}\sum_{j=J_{i-1}+1}^{J_i}\sum_{n=1}^{N} t_{M+n}u(|h_{nj}|^2 q_n) \tag{29a}$$

$$\text{s.t. } Bt_j\log_2\left(1+\frac{|h_{ij}|^2 p_j}{\sigma^2}\right)\geq D_j,\quad \forall i\in\mathcal{N}, j\in\mathcal{J}_i \tag{29b}$$

$$Bt_{M+i}\log_2\left(1+\frac{|h_i|^2 q_i}{\sigma^2}\right)\geq \sum_{j=J_{i-1}+1}^{J_i} D_j,\quad \forall i\in\mathcal{N} \tag{29c}$$

$$t_j\left(\frac{p_j}{\eta}+P^{\mathrm{C}}\right)\leq \sum_{n=1}^{N} t_{M+n}u(|h_{nj}|^2 q_n),\quad \forall i\in\mathcal{N}, j\in\mathcal{J}_i \tag{29d}$$

$$\sum_{i=1}^{N+1} t_i\leq T \tag{29e}$$

$$0\leq p_j\leq P_j, 0\leq q_i\leq Q_i,\quad \forall i\in\mathcal{N}, j\in\mathcal{J}_i \tag{29f}$$

$$\hat{\boldsymbol{t}}\geq \mathbf{0}, \tag{29g}$$

where $\hat{\boldsymbol{t}}=[t_1,\cdots,t_{M+N}]^T$.

Obviously, problem (29) is nonconvex due to nonconvex objective function (29a) and constraints (29b)-(29d). In the following, we first provide the optimal conditions for problem (29), and then we propose a low-complexity algorithm to solve problem (29).

A. Optimal Conditions

Similar to Lemma 1, it is also optimal for each MTCD to transmit with the minimal throughput requirement. Accordingly, the following lemma is directly obtained.

Lemma 3: The optimal solution $(\boldsymbol{p}^*,\boldsymbol{q}^*,\hat{\boldsymbol{t}}^*)$ to problem (29) satisfies

$$Bt_j^*\log_2\left(1+\frac{|h_{ij}|^2 p_j^*}{\sigma^2}\right)=D_j,\quad \forall i\in\mathcal{N}, j\in\mathcal{J}_i. \tag{30}$$

According to (30), the optimal transmission power of MTCD j can be presented as

$$p_j=\frac{1}{|h_{ij}|^2}\left(2^{\frac{D_j}{Bt_j}}-1\right),\quad \forall i\in\mathcal{N}, j\in\mathcal{J}_i. \tag{31}$$

Substituting (31) into (16) yields

$$E_{ij}=\frac{t_j}{|h_{ij}|^2\eta}\left(2^{\frac{D_j}{Bt_j}}-1\right)+t_j P^{\mathrm{C}},\quad \forall i\in\mathcal{N}, j\in\mathcal{J}_i. \tag{32}$$

By analyzing (32), we can obtain the following theorem.

Theorem 5: The energy E_{ij} defined in (32) is convex w.r.t. t_j. When $P^{\mathrm{C}}=0$, the energy E_{ij} monotonically decreases with the transmission time t_j. When $P^{\mathrm{C}}>0$, the energy E_{ij} first decreases with t_j when $0\leq t_j\leq T_{ij}^*$ and then increases with t_j when $t_j>T_{ij}^*$, where T_{ij}^* is the unique zero point of the first-order derivative $\frac{\partial E_{ij}}{\partial t_j}$, i.e.,

$$\left.\frac{\partial E_{ij}}{\partial t_j}\right|_{t_j=T_{ij}^*}=0. \tag{33}$$

Since Theorem 5 can be proved by checking the first-order derivative $\frac{\partial E_{ij}}{\partial t_j}$ as in Appendix B, the proof of Theorem 4 is omitted. Similar to Theorem 2 for NOMA, we come to the similar conclusion for TDMA that transmitting with the maximal transmission time T is optimal when T is not large, while for large T it is not optimal to transmit with the maximal transmission time T.

B. Iterative Power Control and Time Allocation Algorithm

Similar to problem (19), problem (29) has two difficulties: one is the non-smooth EH function in (6), and the other is the nonconvex objective function (29a) and constraints (29b)-(29d). To deal with the first difficulty, we introduce notation $\mathcal{S}_{ij}$ as the set of MTCGs from which MTCD $j\in\mathcal{J}_i$ can effectively harvest energy, i.e., $\mathcal{S}_{ij}=\{n||h_{nj}|^2 q_n>P_0,\forall n\in\mathcal{I}\}$. With $\mathcal{S}_{ij}$ in hand, the harvested power of MTCD $j\in\mathcal{J}_i$ from MTCG $n\in\mathcal{S}_{ij}$ can be presented by the smooth function $\bar{u}(x)$ defined in (28). To tackle the second difficulty, we show that problem (29) with fixed sets $\mathcal{S}_{ij}$'s can be transformed into an equivalent convex problem.

Theorem 6: The original problem in (29) with fixed sets $\mathcal{S}_{ij}$'s can be equivalently transformed into the following convex problem as

$$\min_{\hat{\boldsymbol{p}},\hat{\boldsymbol{q}},\hat{\boldsymbol{t}}} \sum_{i=1}^{N}\sum_{j=J_{i-1}+1}^{J_i}\left(\frac{\hat{p}_j}{\eta}+t_j P^{\mathrm{C}}\right)+\sum_{i=1}^{N}\left(\frac{\hat{q}_i}{\xi}+t_{M+i}Q^{\mathrm{C}}\right) - \sum_{i=1}^{N}\sum_{j=J_{i-1}+1}^{J_i}\sum_{n\in\mathcal{S}_{ij}} t_{M+n}\bar{u}\left(\frac{|h_{nj}|^2\hat{q}_n}{t_{M+n}}\right) \tag{34a}$$

$$\text{s.t. } Bt_j\log_2\left(1+\frac{|h_{ij}|^2\hat{p}_j}{\sigma^2 t_j}\right)\geq D_j,\quad \forall i\in\mathcal{N}, j\in\mathcal{J}_i \tag{34b}$$

$$Bt_{M+i}\log_2\left(1+\frac{|h_i|^2\hat{q}_i}{\sigma^2 t_{M+i}}\right)\geq \sum_{j=J_{i-1}+1}^{J_i} D_j,\quad \forall i\in\mathcal{N} \tag{34c}$$

$$\frac{\hat{p}_j}{\eta}+t_j P^{\mathrm{C}}\leq \sum_{n\in\mathcal{S}_{ij}} t_{M+n}\bar{u}\left(\frac{|h_{nj}|^2\hat{q}_n}{t_{M+n}}\right),\quad \forall i\in\mathcal{N}, j\in\mathcal{J}_i \tag{34d}$$

$$|h_{nj}|^2\hat{q}_n>P_0 t_{M+n},\quad \forall i\in\mathcal{N}, j\in\mathcal{J}_i, n\in\mathcal{S}_{ij} \tag{34e}$$

$$\sum_{i=1}^{N+1} t_i\leq T \tag{34f}$$

$$0\leq\hat{p}_j\leq P_j t_j,\quad \forall i\in\mathcal{N}, j\in\mathcal{J}_i \tag{34g}$$

$$0\leq\hat{q}_i\leq Q_i t_{M+i},\quad \forall i\in\mathcal{N} \tag{34h}$$

$$\hat{\boldsymbol{t}}\geq\mathbf{0}, \tag{34i}$$

where $\hat{\boldsymbol{p}}=[\hat{p}_1,\cdots,\hat{p}_M]^T$ and $\hat{\boldsymbol{q}}=[\hat{q}_1,\cdots,\hat{q}_N]^T$.

Please refer to Appendix F.

Based on Theorem 6, we propose an iterative power control and time allocation for TDMA (IPCTA-TDMA) algorithm with low complexity to obtain a suboptimal solution of problem (29). The idea is to iteratively update sets $\mathcal{S}_{ij}$'s according to the power and time variables obtained in the previous step.

Algorithm 2: Iterative Power Control and Time Allocation for TDMA (IPCTA-TDMA) Algorithm

1: Set $\mathcal{S}_{ij}^{(0)} = \{i\}$, $\forall i \in \mathcal{I}$, $j \in \mathcal{J}_{ij}$, the tolerance θ, the iteration number $v = 0$, and the maximal iteration number $V_{\max}$.
2: **repeat**
3: Obtain the optimal $(\hat{\boldsymbol{p}}^{(v)}, \hat{\boldsymbol{q}}^{(v)}, \hat{\boldsymbol{t}}^{(v)})$ of convex problem (34) with fixed sets $\mathcal{S}_{ij}^{(v)}$.
4: Calculate the objective value (34a) with fixed sets $\mathcal{S}_{ij}^{(v)}$ as $U_{\text{Obj}}^{(v)} = E_{\text{Tot}}(\hat{\boldsymbol{p}}^{(v)}, \hat{\boldsymbol{q}}^{(v)}, \hat{\boldsymbol{t}}^{(v)})$.
5: Set $v = v + 1$.
6: Update $\mathcal{S}_{ij}^{(v)} = \left\{ n \left| \frac{|h_{nj}|^2 \hat{q}_n^{(v-1)}}{t_{M+n}^{(v-1)}} > P_0 \right., \forall n \in \mathcal{I} \right\}$, $\forall i \in \mathcal{I}, j \in \mathcal{J}_i$.
7: **until** $v \geq 2$ and $|U_{\text{Obj}}^{(v)} - U_{\text{Obj}}^{(v-1)}|/U_{\text{Obj}}^{(v-1)} < \theta$ or $v > V_{\max}$.
8: Output $\boldsymbol{p}^* = \hat{\boldsymbol{p}}^{(v)}, \hat{\boldsymbol{t}}^* = \hat{\boldsymbol{t}}^{(v)}, q_i^* = \hat{q}_i^{(v)}/t_{M+i}^{(v)}, \forall i \in \mathcal{I}$.

C. Convergence and Complexity Analysis

Theorem 7: Assuming $V_{\max} \to \infty$, the sequence $(\hat{\boldsymbol{p}}, \hat{\boldsymbol{q}}, \hat{\boldsymbol{t}})$ generated by the IPCTA algorithm converges.

Theorem 7 can be proved by using the same method as in Appendix E. The proof of Theorem 7 is thus omitted.

According to the IPCTA-TDMA algorithm, the major complexity lies in solving the convex problem (34). Considering that the dimension of the variables in problem (34) is $2(M + N)$, the complexity of solving problem (34) by using the standard interior point method is $\mathcal{O}((M + N)^3)$ [57, Pages 487, 569]. As a result, the total complexity of the proposed IPCTA-TDMA algorithm is $\mathcal{O}(L_{\text{TD}}(M + N)^3)$, where L_{TD} denotes the number of iterations of the IPCTA-TDMA algorithm.

V. Numerical Results

In this section, we evaluate the proposed schemes through simulations. There are 40 MTCDs uniformly distributed with a BS in the center. We adopt the "data-centric" clustering technique in [41] for cluster formation of MTCDs, the number of MTCGs is set as 12, and the maximal number of MTCDs associated to one MTCG is 4. For NOMA, all MTCGs are classified into 6 clusters based on the strong-weak scheme [45], [46].

The path loss model is $128.1 + 37.6 \log_{10} d$ (d is in km) and the standard deviation of shadow fading is 4 dB [58]. The noise power $\sigma^2 = -104$ dBm, and the bandwidth of the system is $B = 18$ KHz. For the non-linear EH model in (6), we set $M = 24$ mW, $a = 1500$ and $b = 0.0014$ according to [52], which are obtained by curve fitting from the measurement data in [59]. The receiver sensitivity threshold P_0 is set as

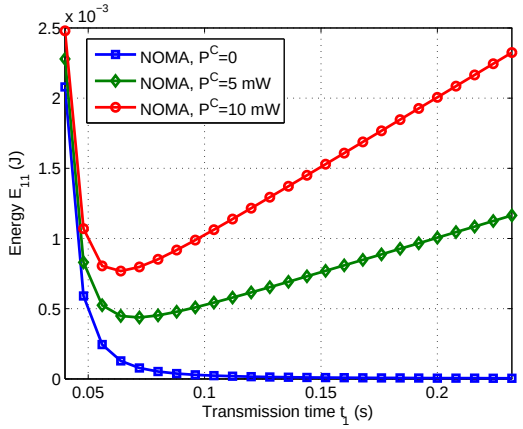

Fig. 6. Energy E_{11} consumed by MTCD 1 versus the transmission time t_1 for NOMA strategy.

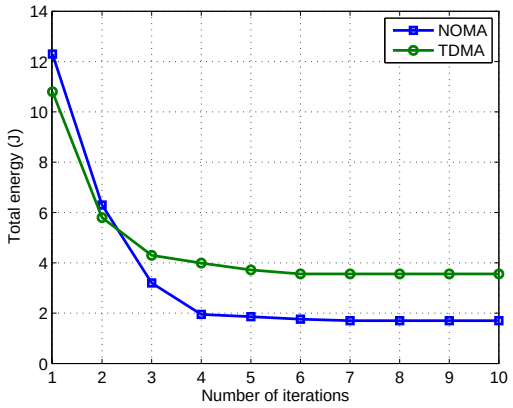

Fig. 7. Convergence behaviors of IPCTA-NOMA and IPATC-TDMA.

0.1 mW. The PA efficiencies of each MTCD and MTCG are set to $\eta = \xi = 0.9$, and the circuit power of each MTCG is $Q^{\text{C}} = 500$ mW as in [55]. We assume equal throughput demand for all MTCDs, i.e., $D_1 = \cdots = D_M = D$, and equal maximal transmission power for each MTCD or MTCG, i.e., $P_1 = \cdots = P_M = P$, and $Q_1 = \cdots = Q_N = Q$. Unless otherwise specified, parameters are set as $P = 5$ mW, $P^{\text{C}} = 0.5$ mW, $Q = 1$ W, $D = 10$ Kbits, and $T = 5$ s.

Fig. 6 depicts, for instance, E_{11} in (23) consumed by MTCD 1 served by MTCG 1 versus the transmission time t_1 for NOMA. It is observed that E_{11} monotonically decreases with t_1 when $P^C = 0$. For the case with $P^C = 5$ mW or $P^C = 10$ mW, E_{11} first decreases and then increases with t_1. Both observations validate our theoretical findings in Theorem 1.

The convergence behaviors of IPCTA-NOMA and IPCTA-TDMA are illustrated in Fig. 7. From this figure, the total energy of both algorithms monotonically decreases, which confirms the convergence analysis in Section III-C and IV-C. It can be seen that both IPCTA-NOMA and IPCTA-TDMA converge rapidly.

In Fig. 8, we illustrate the total energy consumption versus the circuit power of each MTCD. According to Fig. 8, the total energy of NOMA outperforms TDMA when the circuit power of each MTCD is low, i.e., $P^C \leq 4$ mW in the test case. At low circuit power regime, the total energy consumption of the network mainly lies in the RF transmission power of MTCDs and the energy consumed by MTCGs to charge the MTCDs

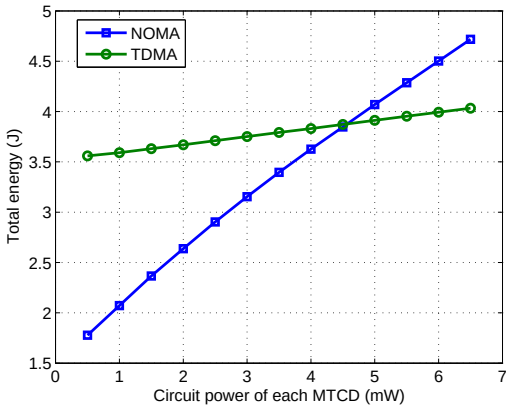

Fig. 8. Total energy versus the circuit power of each MTCD.

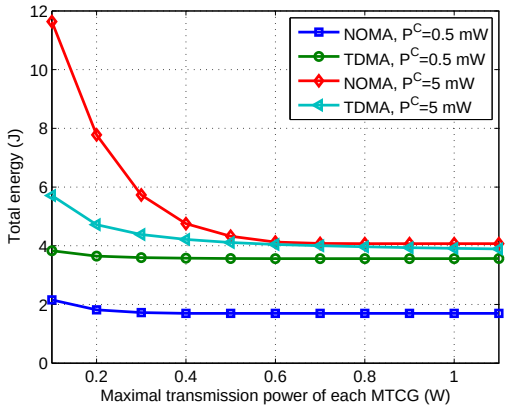

Fig. 9. Total energy versus the maximal transmission power of each MTCG.

through EH. For the NOMA strategy, MTCDs served by the same MTCG can simultaneously upload data and the MTCG decodes the messages according to NOMA detections, which requires lower RF transmission power of MTCDs than the TDMA strategy. Thus, the total energy of NOMA is less than TDMA for low circuit power of each MTCD. From Fig. 8, we can find that the total energy of TDMA outperforms NOMA when the circuit power of each MTCD becomes high, i.e., $P^C \geq 5$ mW in our tests. At high circuit power regime, the total energy consumption of the network mainly lies in the circuit power of MTCDs and the energy consumed by MTCGs to charge the MTCDs through EH. For the NOMA strategy, the transmission time of each MTCD with NOMA is always longer than that with TDMA, which leads to higher circuit power consumption of MTCDs than the TDMA strategy. As a result, TDMA enjoys better energy efficiency than NOMA for high circuit power of each MTCD.

Fig. 9 illustrates the total energy versus the maximal transmission power of each MTCG. It is observed that the total energy decreases with the increase of maximal transmission power of each MTCG for both NOMA and TDMA. This is because that the increment of maximal transmission power of each MTCG allows the MTCG to transmit with large transmission power, which leads to short EH time of MTCDs to harvest enough energy and low total energy consumption of the network. Moreover, it is found that the total energy of NOMA is more sensitive to the maximal transmission power of each MTCG than that of TDMA for high circuit power case as $P^{\mathrm{C}} = 5$ mW for each MTCD. The reason is that MTCD with low channel gain receives intra-cluster interference due to NOMA and the energy consumption is hence especially large for low maximal transmission power of each MTCG and high circuit power of each MTCD.

The total energy versus the maximal transmission power of each MTCD is shown in Fig. 10. It is observed that the total energy decreases with growing maximal transmission power of each MTCD for both NOMA and TDMA. This is due to the fact that a larger maximal transmission power of each MTCD ensures MTCDs can transmit with more power, and the required payload can be uploaded in a shorter time, which results in low circuit power consumption and low energy consumption. It can be found that the total energy of

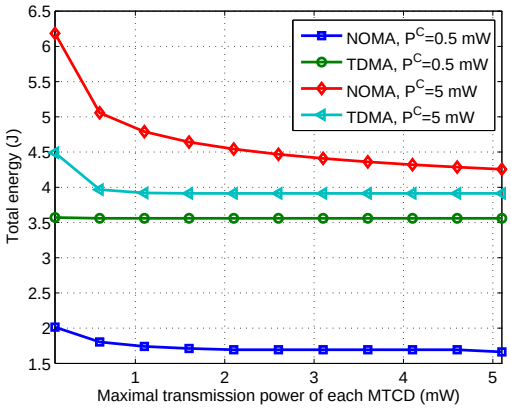

Fig. 10. Total energy versus the maximal transmission power of each MTCD.

TDMA converges faster than that of NOMA as the maximal transmission power of each MTCD increases. This is because that the MTCDs served by the same MTCG simultaneously transmit data for NOMA, and the required transmission power of each MTCD for NOMA is always larger than that of MTCD for TDMA.

Finally, in Fig. 11, we illustrate the total energy versus the required payload of each MTCD. The figure shows that the total energy increases with the required payload of each MTCD. This is due to the fact that large payload of each MTCD requires large energy consumption of MTCDs and MTCGs, which leads to high energy consumption of the network.

VI. Conclusions

This paper compares the total energy consumption between NOMA and TDMA strategies in uplink M2M communications with EH. We formulate the total energy minimization problem subject to minimal throughput constraints, maximal transmission power constraints and energy causality constraints, with the circuit power consumption taken into account. By applying the conditions that it is optimal to transmit with the minimal throughput for each MTCD, we transform the original problem for NOMA strategy into an equivalent problem, which is suboptimally solved through an iterative algorithm. By using a proper variable transformation, we transform the nonconvex problem for TDMA into an equivalent problem, which can

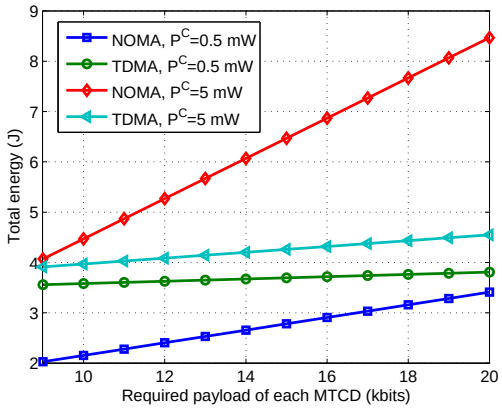

Fig. 11. Total energy versus the required payload of each MTCD.

be effectively solved. Through simulations, either NOMA strategy or TDMA strategy may be preferred depending on different circuit power regimes of MTCDs. At low circuit power regime of MTCDs, NOMA consumes less energy, while TDMA is preferred at high circuit power regime of MTCDs since the energy consumption for NOMA increases significantly as the circuit power of MTCDs increases.

Appendix A
Proof of Lemma 2

By inserting $r_{ij} = D_j$ into (3) from Lemma 1, we have

$$2^{\frac{D_j}{Bt_i}} \sum_{l=j+1}^{J_i} |h_{il}|^2 p_l + \sigma^2 \left(2^{\frac{D_j}{Bt_i}} - 1\right) = \sum_{l=j}^{J_i} |h_{il}|^2 p_l, \quad \text{(A.1)}$$

for $j = J_{i-1}+1, \cdots, J_i$. To solve those $J_i - J_{i-1}$ equations, we first define

$$u_j = \sum_{l=j}^{J_i} |h_{il}|^2 p_l, \quad \forall j \in \mathcal{J}_i. \quad \text{(A.2)}$$

Applying (A.2) into (A.1) yields

$$u_j = 2^{\frac{D_j}{Bt_i}} u_{j+1} + \sigma^2 \left(2^{\frac{D_j}{Bt_i}} - 1\right), \quad \forall j \in \mathcal{J}_i. \quad \text{(A.3)}$$

Denote $\boldsymbol{u}_i = [u_{J_{i-1}+1}, \cdots, u_{J_i}]^T$,

$$\boldsymbol{v}_i = \left[\sigma^2 \left(2^{\frac{D_{J_{i-1}+1}}{Bt_i}} - 1\right), \cdots, \sigma^2 \left(2^{\frac{D_{J_i}}{Bt_i}} - 1\right)\right]^T, \quad \text{(A.4)}$$

and

$$\boldsymbol{W}_i = \begin{bmatrix} 0 & 2^{\frac{D_{J_{i-1}+1}}{Bt_i}} & & & \\ & 0 & 2^{\frac{D_{J_{i-1}+2}}{Bt_i}} & & \\ & & \ddots & \ddots & \\ & & & 0 & 2^{\frac{D_{J_i-1}}{Bt_i}} \\ & & & & 0 \end{bmatrix}. \quad \text{(A.5)}$$

Equations in (A.3) can be rewritten as

$$(\boldsymbol{E} - \boldsymbol{W}_i)\boldsymbol{u}_i = \boldsymbol{v}_i, \quad \text{(A.6)}$$

where $\boldsymbol{E}$ is an identity matrix of size $(J_i - J_{i-1}) \times (J_i - J_{i-1})$. From (A.6), we have

$$\boldsymbol{u}_i = (\boldsymbol{E} - \boldsymbol{W}_i)^{-1} \boldsymbol{v}_i. \quad \text{(A.7)}$$

Before obtaining the inverse matrix $(\boldsymbol{E} - \boldsymbol{W}_i)^{-1}$, we present the following lemma.

Lemma 4: When $l \in [1, J_i - J_{i-1} - 1]$, the l-th power of matrix $\boldsymbol{W}_i$ can be expressed as

$$\boldsymbol{W}_i^l = \begin{bmatrix} \boldsymbol{0}_l^T & 2^{\frac{\sum_{s=J_{i-1}+1}^{J_{i-1}+l} D_s}{Bt_i}} & & & \\ & 0 & 2^{\frac{\sum_{s=J_{i-1}+2}^{J_{i-1}+l+1} D_s}{Bt_i}} & & \\ & & \ddots & \ddots & \\ & & & 0 & 2^{\frac{\sum_{s=J_i-l}^{J_i-1} D_s}{Bt_i}} \\ & & & & \boldsymbol{0}_l \end{bmatrix}, \quad \text{(A.8)}$$

where $\boldsymbol{0}_l$ denotes a $l \times 1$ vector of zeros. When $l = J_i - J_{i-1}$, $\boldsymbol{W}_i^l = \boldsymbol{0}_{(J_i - J_{i-1}) \times (J_i - J_{i-1})}$, where $\boldsymbol{0}_{(J_i - J_{i-1}) \times (J_i - J_{i-1})}$ is a $(J_i - J_{i-1}) \times (J_i - J_{i-1})$ matrix of zeros.

Lemma 4 can be proved by the principle of mathematical induction.

Basis: It can be verified that Lemma 4 is valid for $l = 1$.

Induction Hypothesis: For $l \in [1, J_i - J_{i-1} - 2]$, assume that the l-th power of matrix $\boldsymbol{W}_i$ can be expressed as (A.8).

Induction Step: According to (A.8), we can obtain

$$\begin{aligned} \boldsymbol{W}_i^{l+1} &= \boldsymbol{W}_i^l \boldsymbol{W}_i \\ &= \begin{bmatrix} \boldsymbol{0}_l^T & 2^{\frac{\sum_{s=J_{i-1}+1}^{J_{i-1}+l} D_s}{Bt_i}} & & & \\ & 0 & 2^{\frac{\sum_{s=J_{i-1}+2}^{J_{i-1}+l+1} D_s}{Bt_i}} & & \\ & & \ddots & \ddots & \\ & & & 0 & 2^{\frac{\sum_{s=J_i-l}^{J_i-1} D_s}{Bt_i}} \\ & & & & \boldsymbol{0}_l \end{bmatrix} \\ &\quad \cdot \begin{bmatrix} 0 & 2^{\frac{D_{J_{i-1}+1}}{Bt_i}} & & & \\ & 0 & 2^{\frac{D_{J_{i-1}+2}}{Bt_i}} & & \\ & & \ddots & \ddots & \\ & & & 0 & 2^{\frac{D_{J_i-1}}{Bt_i}} \\ & & & & 0 \end{bmatrix} \\ &= \begin{bmatrix} \boldsymbol{0}_{l+1}^T & 2^{\frac{\sum_{s=J_{i-1}+1}^{J_{i-1}+l+1} D_s}{Bt_i}} & & & \\ & 0 & 2^{\frac{\sum_{s=J_{i-1}+2}^{J_{i-1}+l+2} D_s}{Bt_i}} & & \\ & & \ddots & \ddots & \\ & & & 0 & 2^{\frac{\sum_{s=J_i-l-1}^{J_i-1} D_s}{Bt_i}} \\ & & & & \boldsymbol{0}_{l+1} \end{bmatrix}, \end{aligned}$$

which verifies that the $(l+1)$-th power of matrix $\boldsymbol{W}_i$ can also be expressed as (A.8). According to (A.8) and (A.5), it is verified that

$$\boldsymbol{W}_i^{J_i - J_{i-1}} = \boldsymbol{W}_i^{J_i - J_{i-1} - 1} \boldsymbol{W}_i = \boldsymbol{0}_{(J_i - J_{i-1}) \times (J_i - J_{i-1})}. \quad \text{(A.9)}$$

Therefore, Lemma 4 is proved.

Now, it is ready to obtain the inverse matrix $(\boldsymbol{E}-\boldsymbol{W}_i)^{-1}$. Since

$$(\boldsymbol{E}-\boldsymbol{W}_i)\left(\boldsymbol{E}+\sum_{l=1}^{J_i-J_{i-1}-1}\boldsymbol{W}_i^l\right)=\boldsymbol{E}-\boldsymbol{W}_i^{J_i-J_{i-1}}=\boldsymbol{E}, \tag{A.10}$$

we have

$$(\boldsymbol{E}-\boldsymbol{W}_i)^{-1}=\boldsymbol{E}+\sum_{l=1}^{J_i-J_{i-1}-1}\boldsymbol{W}_i^l. \tag{A.11}$$

Substituting (A.8) and (A.11) into (A.7) yields

$$u_j=\sum_{l=j}^{J_i}\sigma^2\left(2^{\frac{D_l}{Bt_i}}-1\right)2^{\frac{\sum_{s=j}^{l-1}D_s}{Bt_i}},\quad \forall j\in\mathcal{J}_i, \tag{A.12}$$

where we define $\prod_{s=j}^{j-1}2^{\frac{D_s}{Bt_i}}=2^0$. From (A.12), we can obtain $u_j=\sigma^2\left(2^{\frac{\sum_{s=j}^{J_i}D_s}{Bt_i}}-1\right)$. Since $\sum_{l=J_i+1}^{J_i}p_j=0$, we have

$$u_{J_i+1}=0. \tag{A.13}$$

From (A.2) and (A.13), we can obtain the transmission power of MTCD j as

$$p_{ij}=\frac{u_j-u_{j+1}}{|h_{ij}|^2},\quad \forall j\in\mathcal{J}_i. \tag{A.14}$$

Applying (A.12) and (A.13) to (A.14), we have

$$\begin{aligned}
p_j=&\sum_{l=j}^{J_i}\frac{\sigma^2}{|h_{ij}|^2}\left(2^{\frac{D_l}{Bt_i}}-1\right)2^{\frac{\sum_{s=j}^{l-1}D_s}{Bt_i}}\\
&-\sum_{l=j+1}^{J_i}\frac{\sigma^2}{|h_{ij}|^2}\left(2^{\frac{D_l}{Bt_i}}-1\right)2^{\frac{\sum_{s=j+1}^{l-1}D_s}{Bt_i}}\\
=&\sum_{l=j+1}^{J_i}\frac{\sigma^2}{|h_{ij}|^2}\left(2^{\frac{D_l}{Bt_i}}-1\right)\left(2^{\frac{D_j}{Bt_i}}-1\right)2^{\frac{\sum_{s=j+1}^{l-1}D_s}{Bt_i}}\\
&+\frac{\sigma^2}{|h_{ij}|^2}\left(2^{\frac{D_j}{Bt_i}}-1\right)2^{\frac{\sum_{s=j}^{j-1}D_s}{Bt_i}},\\
=&\sum_{l=j+1}^{J_i}\frac{\sigma^2}{|h_{ij}|^2}\left(\mathrm{e}^{\frac{a_l}{t_i}}-1\right)\left(\mathrm{e}^{\frac{a_j}{t_i}}-1\right)\mathrm{e}^{\frac{b_{jl}}{t_i}}\\
&+\frac{\sigma^2}{|h_{ij}|^2}\left(\mathrm{e}^{\frac{a_j}{t_i}}-1\right),\quad \forall j\in\mathcal{J}_i.
\end{aligned} \tag{A.15}$$

where a_l and b_{jl} are defined in (22). Since e^x-1 with $x\geq 0$ is non-negative and decreases with t_i, p_j is also non-negative and decreases with t_i from (A.15).

Appendix B
Proof of Theorem 1

To show that the energy E_{ij} is convex w.r.t. t_i, we first define function

$$f_{ijl}(x)=(\mathrm{e}^{a_l x}-1)(\mathrm{e}^{a_j x}-1)\mathrm{e}^{b_{jl}x},\quad \forall x\geq 0. \tag{B.1}$$

Then, the second-order derivative follows

$$\begin{aligned}
f''_{ijl}(x)=&(a_l^2+2a_lb_{jl})(\mathrm{e}^{a_jx}-1)\mathrm{e}^{(a_l+b_{jl})x}\\
&+2a_la_j\mathrm{e}^{(a_l+a_j+b_{jl})x}\\
&+(a_j^2+2a_jb_{jl})(\mathrm{a}^{a_lx}-1)\mathrm{e}^{(a_j+b_{jl})x}\\
&+b_{jl}^2(\mathrm{e}^{a_lx}-1)(\mathrm{e}^{a_jx}-1)\mathrm{e}^{b_{jl}x}\geq 0,
\end{aligned} \tag{B.2}$$

which indicates that $f_{ijl}(x)$ is convex w.r.t. x. According to [57, Page 89], the perspective of $u(x)$ is the function $v(x,t)$ defined by $v(x,t)=tu(x/t)$, **dom** $v=\{(x,t)|x/t\in$ **dom** $u, t>0\}$. If $u(x)$ is a convex function, then so is its perspective function $v(x,t)$ [57, Page 89]. Since $f_{ijl}(x)$ is convex, the perspective function

$$\bar{f}_{ijl}(x,t_i)=t_if_{ijl}\left(\frac{x}{t_i}\right) \tag{B.3}$$

is convex w.r.t. (x,t_i). Thus, function $\bar{f}_{ijl}(1,t_i)$ is also convex w.r.t. t_i.

Defining function

$$g_{ij}(x)=\mathrm{e}^{a_jx}-1, \tag{B.4}$$

which is convex w.r.t. x. By using the property of perspective function [57, Page 89], we also have that function

$$\bar{g}_{ij}(x,t_i)=t_ig_{ij}\left(\frac{x}{t_i}\right) \tag{B.5}$$

is convex w.r.t. (x,t_i) and function $\bar{g}_{ij}(1,t_i)$ is accordingly convex w.r.t. t_i.

Substituting (B.3) and (B.5) into (23), we can obtain

$$E_{ij}=\sum_{l=j+1}^{J_i}\frac{\sigma^2}{\eta|h_{ij}|^2}\bar{f}_{ijl}(1,t_i)+\frac{\sigma^2}{\eta|h_{ij}|^2}\bar{g}_{ij}(1,t_i)+t_iP_{\mathrm{C}}. \tag{B.6}$$

Due to the fact that both $\bar{f}_{ijl}(1,t_i)$ and $\bar{g}_{ij}(1,t_i)$ are convex, E_{ij} is consequently convex w.r.t. t_i from (B.6).

According to (23), the first-order derivative of E_i w.r.t. t_i is expressed as

$$\begin{aligned}
\frac{\partial E_{ij}}{\partial t_i}=&\sum_{l=j+1}^{J_i}\frac{\sigma^2}{\eta|h_{ij}|^2}\left(\mathrm{e}^{\frac{a_l}{t_i}}-1\right)\left(\mathrm{e}^{\frac{a_j}{t_i}}-1\right)\mathrm{e}^{\frac{b_{jl}}{t_i}}\\
&-\sum_{l=j+1}^{J_i}\frac{\sigma^2a_l}{\eta|h_{ij}|^2t_i}\left(\mathrm{e}^{\frac{a_j}{t_i}}-1\right)\mathrm{e}^{\frac{a_l+b_{jl}}{t_i}}\\
&-\sum_{l=j+1}^{J_i}\frac{\sigma^2a_j}{\eta|h_{ij}|^2t_i}\left(\mathrm{e}^{\frac{a_l}{t_i}}-1\right)\mathrm{e}^{\frac{a_j+b_{jl}}{t_i}}\\
&-\sum_{l=j+1}^{J_i}\frac{\sigma^2b_{jl}}{\eta|h_{ij}|^2t_i}\left(\mathrm{e}^{\frac{a_l}{t_i}}-1\right)\left(\mathrm{e}^{\frac{a_j}{t_i}}-1\right)\mathrm{e}^{\frac{b_{jl}}{t_i}}\\
&+\frac{\sigma^2}{\eta|h_{ij}|^2}\left(\mathrm{e}^{\frac{a_j}{t_i}}-1\right)-\frac{\sigma^2a_j}{\eta|h_{ij}|^2t_i}\mathrm{e}^{\frac{a_j}{t_i}}+P_{\mathrm{C}}.
\end{aligned} \tag{B.7}$$

Since E_{ij} is convex w.r.t. t_i, function $\frac{\partial E_{ij}}{\partial t_i}$ increases with t_i. Because D_j is positive for all j, we have $a_l>0$, $b_{ijl}>0$ and

$c_{ijl} > 0$ from (22). To calculate the limit of $\frac{\partial E_{ij}}{\partial t_i}$ at $t_i = 0+$, we calculate the following limit,

$$\begin{aligned}
&\lim_{t_i \to 0+} \frac{\sigma^2}{\eta |h_{ij}|^2} \left(\mathrm{e}^{\frac{a_l}{t_i}} - 1\right) \left(\mathrm{e}^{\frac{a_j}{t_i}} - 1\right) \mathrm{e}^{\frac{b_{jl}}{t_i}} \\
&\quad - \frac{\sigma^2 a_l}{\eta |h_{ij}|^2 t_i} \left(\mathrm{e}^{\frac{a_j}{t_i}} - 1\right) \mathrm{e}^{\frac{a_l + b_{jl}}{t_i}} \\
&= \lim_{x \to +\infty} \frac{\sigma^2}{\eta |h_{ij}|^2} \left(\mathrm{e}^{a_l x} - 1\right) \left(\mathrm{e}^{a_j x} - 1\right) \mathrm{e}^{b_{jl} x} \\
&\quad - \frac{\sigma^2 a_l x}{\eta |h_{ij}|^2} \left(\mathrm{e}^{a_j x} - 1\right) \mathrm{e}^{(a_l + b_{jl}) x} \\
&= \lim_{x \to +\infty} \frac{\sigma^2 (1 - a_l x)}{\eta |h_{ij}|^2} \mathrm{e}^{(a_l + a_j + b_{jl}) x} \\
&= -\infty. \qquad \text{(B.8)}
\end{aligned}$$

Thus, when t_i approaches zero in the positive direction, we have

$$\lim_{t_i \to 0+} \frac{\partial E_{ij}}{\partial t_i} = -\infty. \qquad \text{(B.9)}$$

When t_i approaches positive infinity, the limit of first-order derivative $\frac{\partial E_{ij}}{\partial t_i}$ can be calculated as

$$\lim_{t_i \to +\infty} \frac{\partial E_{ij}}{\partial t_i} = P_{\mathrm{C}}. \qquad \text{(B.10)}$$

If $P_{\mathrm{C}} = 0$, then $\frac{\partial E_{ij}}{\partial t_i} \leq 0$ for all $t_i \geq 0$. In this case, the energy E_{ij} always decreases with t_i. If $P_{\mathrm{C}} > 0$, we can observe that $\lim_{t_i \to +\infty} \frac{\partial E_{ij}}{\partial t_i} > 0$ from (B.10). Since $\lim_{t_i \to 0+} \frac{\partial E_{ij}}{\partial t_i} < 0$ and $\frac{\partial E_{ij}}{\partial t_i}$ increases with t_i, there exists one unique solution T_{ij}^* satisfying (24), which can be solved by using the bisection method. In particular, E_{ij} decreases with $0 \leq t_i \leq T_{ij}^*$ and increases with $t_{ij} > T_{ij}^*$.

Appendix C
Proof of Theorem 2

We first consider the case that $T \leq \max_{\forall i \in \mathcal{N}} \min_{\forall j \in \mathcal{J}_i} \{T_{ij}^*\}$. Without loss of generality, we denote $T \leq T_{nm}^* = \max_{\forall i \in \mathcal{N}} \min_{\forall j \in \mathcal{J}_i} \{T_{ij}^*\}$. Assume that the optimal solution $(\boldsymbol{p}^*, \boldsymbol{q}^*, \boldsymbol{t}^*)$ to problem (19) satisfies $\sum_{i=1}^{N+K} t_i^* < T$. Due to that $t_i^* \geq 0$ for all i, we can obtain that $t_n^* \leq T_{nm}^* \leq T_{nl}^*$, $\forall l \in \mathcal{J}_n$. With all other power p_j^*, q_i^* and time t_k^* fixed, $j \in \mathcal{M} \setminus \mathcal{J}_n$, $i \in \mathcal{N}$, $k \in \mathcal{N} \setminus \{n\}$, we increase the time t_n^* to $t_n' = t_n^* + \epsilon$ by an arbitrary amount $(0, T - \sum_{i=1, i \neq n}^{N} t_i^*]$. Using (21), the corresponding power p_l^* strictly deceases to p_l', $l \in \mathcal{J}_n$. According to Theorem 1, the energy E_{nl} decreases with the transmission time $0 \leq t_n \leq T_{nl}^*$, $\forall l \in \mathcal{J}_n$. As a result, with new power-time pair $(p'_{J_{n-1}+1}, \cdots, p'_{J_n}, t_n')$, the objective function (19a) decreases with all the constraints satisfied. By contradiction, we must have $\sum_{i=1}^{N+K} t_i^* = T$ for the optimal solution. This completes the proof of the first half part of Theorem 2.

The last half part of Theorem 2 indicates that transmitting with maximal transmission time is not optimal when T is larger than a threshold T_{Upp}. This can be proved by using the contradiction method. Specifically, assuming that total transmission time of the optimal solution is the maximal transmission time T, we can find a special solution with total transmission time less than T, which strictly outperforms the optimal solution. To obtain the threshold T_{Upp}, we consider a special solution that satisfies all the constraints of problem (19) except the maximal transmission time constraint (19e).

Since E_{ij} is convex w.r.t. t_i according to Theorem 1, the energy $E_i = \sum_{j=J_{i-1}+1}^{J_i} E_{ij}$ consumed by all MTCDs in $\mathcal{J}_i$ served by MTCG i is also convex w.r.t. t_i. Based on the proof of Theorem 1, we directly obtain the following lemma.

Lemma 5: The energy E_i consumed by all MTCDs in $\mathcal{J}_i$ first decreases with the transmission time t_i when $0 \leq t_i \leq T_i^*$ and then increases with the transmission time t_i when $t_i > T_i^*$, where T_i^* is the unique zero point of first-order derivative $\frac{\partial E_i}{\partial t_i}$, i.e.,

$$\left.\frac{\partial E_i}{\partial t_i}\right|_{t_i = T_i^*} = \sum_{j=J_{i-1}+1}^{J_i} \left.\frac{\partial E_{ij}}{\partial t_i}\right|_{t_i = T_i^*} = 0. \qquad \text{(C.1)}$$

Since Lemma 5 can be proved by checking the first-order derivative $\frac{\partial E_i}{\partial t_i}$ as in Appendix B, the proof of Lemma 5 is omitted here.

Set $\tilde{t}_i = T_i^*$, and $\tilde{p}_j$ can be obtained from (21) with $\tilde{t}_i$, $i \in \mathcal{N}$, $j \in \mathcal{J}_i$. For the transmission power of the MTCGs, we set $\tilde{q}_i = Q_i$, $i \in \mathcal{N}$. Denote $\tilde{\boldsymbol{p}} = [\tilde{p}_1, \cdots, \tilde{p}_M]^T$, $\tilde{\boldsymbol{q}} = [\tilde{q}_1, \cdots, \tilde{q}_N]^T$. With power $(\tilde{\boldsymbol{p}}, \tilde{\boldsymbol{q}})$ and time $(\tilde{t}_i, \cdots, \tilde{t}_N)$ fixed for now, the energy minimization problem (19) without constraint (19e) becomes

$$\begin{aligned}
\min_{\boldsymbol{\tau}} \; & \sum_{k=1}^{K} \sum_{i=I_{k-1}+1}^{I_k} t_{N+k} \left(\frac{Q_i}{\xi} + Q^{\mathrm{C}}\right) \\
& - \sum_{k=1}^{K} \sum_{i=1}^{N} \sum_{j=J_{i-1}+1}^{J_i} t_{N+1} u \left(\sum_{n=J_{k-1}+1}^{J_k} |h_{nj}|^2 Q_n\right) \qquad \text{(C.2a)} \\
\text{s.t.} \; & B t_{N+i} \log_2 \left(1 + \frac{|h_i|^2 Q_i}{\sum_{n=i+1}^{I_k} |h_n|^2 Q_n + \sigma^2}\right) \geq \sum_{j \in \mathcal{J}_i} D_j, \\
& \qquad \forall k \in \mathcal{K}, i \in \mathcal{I}_k \qquad \text{(C.2b)} \\
& \tilde{t}_i \left(\frac{\tilde{p}_j}{\eta} + P^{\mathrm{C}}\right) \leq \sum_{k=1}^{K} t_{N+k} u \left(\sum_{n=I_{k-1}+1}^{I_k} |h_{nj}|^2 Q_n\right), \\
& \qquad \forall i \in \mathcal{N}, j \in \mathcal{J}_i \qquad \text{(C.2c)} \\
& \boldsymbol{\tau} \geq \mathbf{0}, \qquad \text{(C.2d)}
\end{aligned}$$

where $\boldsymbol{\tau} = [t_{N+1}, \cdots, t_{N+K}]^T$. Problem (C.2) can be obtained by substituting (11) into (19a), (4) into (19b), and (5) and (7) into (19c). Problem (C.2) is a linear problem, which can be optimally solved via the simplex method. Denote the optimal solution of problem by $\boldsymbol{\tau}^* = [T_{N+1}^*, \cdots, T_{N+K}^*]^T$. Denote $\tilde{t}_{N+k} = T_{N+k}^*$, $\forall k \in \mathcal{K}$, and $\tilde{\boldsymbol{t}} = [\tilde{t}_1, \cdots, \tilde{t}_{N+K}]^T$. As a result, we obtain a special solution $(\tilde{\boldsymbol{p}}, \tilde{\boldsymbol{q}}, \tilde{\boldsymbol{t}})$ that satisfies all the constraints of problem (19) except the maximal transmission time constraint (19e). With solution $(\tilde{\boldsymbol{p}}, \tilde{\boldsymbol{q}}, \tilde{\boldsymbol{t}})$, the total energy consumption $\tilde{E}_{\text{Tot}}$ obtained from (11) can be expressed

as

$$\begin{aligned}\tilde{E}_{\text{Tot}} &= \sum_{i=1}^{N+K} \tilde{E}_i \\ &= \sum_{i=1}^{N} \sum_{j=J_{i-1}+1}^{J_i} \tilde{t}_i \left(\frac{\tilde{p}_j}{\eta} + P^{\text{C}} \right) \\ &\quad + \sum_{k=1}^{K} \sum_{i=I_{k-1}+1}^{I_k} \tilde{t}_{N+k} \left(\frac{\tilde{q}_i}{\xi} + Q^{\text{C}} \right) \\ &\quad - \sum_{k=1}^{K} \sum_{i=1}^{N} \sum_{j=J_{i-1}+1}^{J_i} \tilde{t}_{N+k} u \left(\sum_{n=I_{k-1}+1}^{I_k} |h_{nj}|^2 \tilde{q}_n \right), \end{aligned} \tag{C.3}$$

where $\tilde{E}_i$ is the energy consumed by all MTCDs in $\mathcal{J}_i$, $i \in \mathcal{N}$, and $\tilde{E}_{N+k}$ is the system energy consumption during the $(N+k)$-th phase.

Denote an upper bound of maximal transmission time by

$$T_{\text{Upp}} = \max \left\{ \sum_{i=1}^{N+K} T_i^*, T_{\text{Amp}} \right\}, \tag{C.4}$$

where

$$T_{\text{Amp}} = \frac{\left(1 + \sum_{i=1}^{N} \beta_i\right) \sum_{k=1}^{K} \tilde{E}_{N+k}}{\alpha Q^{\text{C}}}, \tag{C.5}$$

with α defined in (C.8) and β_i defined in (C.11). If $T \geq T_{\text{Upp}}$, we show that optimal solution $(\boldsymbol{p}^*, \boldsymbol{q}^*, \boldsymbol{t}^*)$ to problem (19) must satisfy constraint (26), i.e., (19e) is inactive, by contradiction. Assume that

$$\sum_{i=1}^{N+K} t_i^* = T. \tag{C.6}$$

With $(\boldsymbol{p}^*, \boldsymbol{q}^*, \boldsymbol{t}^*)$, we denote E_i^* as the energy consumed by all MTCDs in $\mathcal{J}_i$, $i \in \mathcal{N}$, E_{N+k}^* as the system energy consumption during the $(N+k)$-th phase, and E_{Tot}^* as the total energy of the whole system. Thus, we have

$$\begin{aligned} E_{\text{Tot}}^* &= \sum_{i=1}^{N+K} E_i^* \\ &\overset{\text{(a)}}{\geq} \sum_{i=1}^{N+1} \tilde{E}_i + \sum_{k=1}^{K} E_{N+k}^* \\ &\overset{\text{(b)}}{=} \sum_{i=1}^{N} \tilde{E}_i + \sum_{k=1}^{K} t_{N+k}^* \left(\sum_{n=I_{k-1}+1}^{I_k} \frac{q_n^*}{\xi} - \sum_{i=1}^{N} \sum_{j=J_{i-1}+1}^{J_i} \right. \\ &\quad \left. u \left(\sum_{n=I_{k-1}+1}^{I_k} |h_{nj}|^2 q_n^* \right) \right) + Q^{\text{C}} \sum_{k=1}^{K} t_{N+k}^* (I_k - I_{k-1}) \\ &\overset{\text{(c)}}{>} \sum_{i=1}^{N} \tilde{E}_i + \alpha Q^{\text{C}} \sum_{k=1}^{K} t_{N+k}^* \\ &\overset{\text{(d)}}{\geq} \sum_{i=1}^{N+K} \tilde{E}_i = \tilde{E}_{\text{Tot}}, \end{aligned} \tag{C.7}$$

where inequality (a) follows from the fact that E_i achieves the minimum when $t_i = T_i^*$ according to Lemma 5, equality (b) holds from (5) and (9), and inequality (c) follows from (5), (10), $\xi \in (0, 1]$ and

$$\alpha \triangleq \min_{k \in \mathcal{K}} (I_k - I_{k-1}). \tag{C.8}$$

To explain procedure (d), we substitute (5) and (7) into energy causality constraints (19d) to obtain

$$t_i^* \left(\frac{p_j^*}{\eta} + P^{\text{C}} \right) \leq \sum_{k=1}^{K} t_{N+k}^* u \left(\sum_{n=I_{k-1}+1}^{I_k} |h_{nj}|^2 q_n \right), \tag{C.9}$$

for all $i \in \mathcal{N}, j \in \mathcal{J}_i$.

Considering that $p_j^* \geq 0$ in the left hand side of (C.9) and $u(x)$ is a increasing function as well as $q_i^* \leq Q_i$ in the right hand side of (C.9), we have

$$\begin{aligned} t_i^* &\leq \min_{j \in \mathcal{J}_i} \left\{ \frac{\sum_{k=1}^{K} t_{N+k}^* u \left(\sum_{n=I_{k-1}+1}^{I_k} |h_{nj}|^2 Q_n \right)}{P^C} \right\}, \\ &\leq \beta_i \sum_{k=1}^{K} t_{N+k}^*, \quad \forall i \in \mathcal{N}, \end{aligned} \tag{C.10}$$

where

$$\beta_i = \min_{j \in \mathcal{J}_i} \left\{ \max_{k \in \mathcal{K}} \frac{u \left(\sum_{n=I_{k-1}+1}^{I_k} |h_{nj}|^2 Q_n \right)}{P^C} \right\}. \tag{C.11}$$

Combining (C.6) and (C.8) yields

$$\sum_{k=1}^{K} t_{N+k}^* \geq \frac{T}{1 + \sum_{i=1}^{N} \beta_i}. \tag{C.12}$$

Hence, inequality (d) follows from (C.4) and (C.12).

According to (C.2) and (C.4), solution $(\tilde{\boldsymbol{p}}, \tilde{\boldsymbol{q}}, \tilde{\boldsymbol{t}})$ is a feasible solution to problem (19). From (C.7), the objective value (19a) can be decreased with solution $(\tilde{\boldsymbol{p}}, \tilde{\boldsymbol{q}}, \tilde{\boldsymbol{t}})$, which contradicts that $(\boldsymbol{p}^*, \boldsymbol{q}^*, \boldsymbol{t}^*)$ is the optimal solution to problem (19). Hence, the optimal solution to problem (19) must satisfy constraint (26).

Appendix D
Proof of Theorem 3

We first show that the feasible set of problem (27) with given $\boldsymbol{\tau}$ is convex. Obviously, constraints (27b), (27d), (27e) and (27g) and (27h) are all linear w.r.t. $(\boldsymbol{q}, \bar{\boldsymbol{t}})$. According to (B.1) and (B.3), constraints (27c) and (27f) can be, respectively, reformulated as

$$\sum_{l=j+1}^{J_i} \bar{f}_{ijl}(1, t_i) + t_i P^{\text{C}} \leq \sum_{k \in \mathcal{S}_{ij}} t_{N+k} \bar{u} \left(\sum_{n=I_{k-1}+1}^{I_k} |h_{nj}|^2 q_n \right) \tag{D.1}$$

for all $i \in \mathcal{N}, j \in \mathcal{J}_i$, and

$$\sum_{l=j+1}^{J_i} f_{ijl} \left(\frac{1}{t_i} \right) \leq P_j, \quad \forall i \in \mathcal{N}, j \in \mathcal{J}_i. \tag{D.2}$$

Based on (28), we have

$$\bar{u}''(x) = \frac{-Ma^2(1 + \mathrm{e}^{ab})\mathrm{e}^{-a(x-b)}}{\mathrm{e}^{ab}(1 + \mathrm{e}^{-a(x-b)})^3} \leq 0, \quad \forall x \geq 0, \tag{D.3}$$

which shows that $\bar{u}(x)$ is concave, and $-\bar{u}(x)$ is convex. Since $\bar{f}_{ijl}(1,t_i)$ is convex w.r.t. t_i according to Appendix B, constraints (D.1) are convex, i.e., constraints (27c) are convex. Due to that $f_{ijl}(x)$ is convex and non-decreasing, and $\frac{1}{x}$ is convex, $f_{ijl}\left(\frac{1}{x}\right)$ is also convex according to the composition property of convex functions [57, Page 84]. Thus, constraints (D.2) are convex, i.e., constraints (27f) are convex.

We then show that the objective function (27a) is convex. Substituting (B.3) and (B.5) into (27a) yields

$$\begin{aligned}
&\sum_{i=1}^{N}\sum_{j=J_{i-1}+1}^{J_i}\sum_{l=j+1}^{J_i}\frac{\sigma^2}{\eta|h_{ij}|^2}\bar{f}_{ijl}(1,t_i)\\
&+\sum_{i=1}^{N}\sum_{j=J_{i-1}+1}^{J_i}\frac{\sigma^2}{\eta|h_{ij}|^2}\bar{g}_{ij}(1,t_i)\\
&+\sum_{i=1}^{N}\sum_{j=J_{i-1}+1}^{J_i}t_iP_{\mathrm{C}}+\sum_{k=1}^{K}\sum_{i=I_{k-1}+1}^{I_k}t_{N+k}\left(\frac{q_i}{\xi}+Q^{\mathrm{C}}\right)\\
&-\sum_{i=1}^{N}\sum_{j=J_{i-1}+1}^{J_i}\sum_{k\in\mathcal{S}_{ij}}t_{N+k}\bar{u}\left(\sum_{n=I_{k-1}+1}^{I_k}|h_{nj}|^2q_n\right), \quad \text{(D.4)}
\end{aligned}$$

which is convex w.r.t. $(\boldsymbol{q},\bar{\boldsymbol{t}})$ because $\bar{f}_{ijl}(1,t_i)$, $\bar{g}_{ij}(1,t_i)$ and $-\bar{u}(x)$ are convex according to Appendix B and (D.3). As a result, problem (27) is convex w.r.t. $(\boldsymbol{q},\bar{\boldsymbol{t}})$.

With given $(\boldsymbol{q},\bar{\boldsymbol{t}})$, constraints (27b) can be equivalently transformed into

$$Bt_{N+i}\log_2\left(1+\frac{|h_i|^2q_i}{\sum_{n=i+1}^{I_k}|h_n|^2q_n+\sigma^2}\right)\geq\sum_{j=J_{i-1}+1}^{J_i}D_j, \quad \text{(D.5)}$$

which is linear w.r.t. t_{N+i}. By replacing constraints (27b) with (D.5), problem (27) with given $(\boldsymbol{q},\bar{\boldsymbol{t}})$ is a linear problem.

Appendix E
Proof of Theorem 4

The proof is established by showing that the total energy value (27a) is non-increasing when sequence $(\boldsymbol{q},\boldsymbol{t})$ is updated. According to the IPCTA-NOMA algorithm, we have

$$U_{\mathrm{Obj}}^{(v-1)}=E_{\mathrm{Tot}}(\boldsymbol{q}^{(v-1)},\boldsymbol{t}^{(v-1)})\geq E_{\mathrm{Tot}}(\boldsymbol{q}^{(v)},\boldsymbol{t}^{(v)})=U_{\mathrm{Obj}}^{(v)}, \quad \text{(E.1)}$$

where the inequality follows from that $(\boldsymbol{q}^{(v)},\boldsymbol{t}^{(v)})$ is a suboptimally optimal solution of problem (27) with fixed sets $\mathcal{S}_{ij}^{(v)}$, while $(\boldsymbol{q}^{(v-1)},\boldsymbol{t}^{(v-1)})$ is the initial feasible solution of problem (34) with fixed sets $\mathcal{S}_{ij}^{(v)}$. Furthermore, the total energy value (27a) is always non-negative. Since the total energy value (27a) is non-increasing in each iteration according to (E.1) and the total energy value (27a) is finitely lower-bounded, the IPCTA-NOMA algorithm must converge.

Appendix F
Proof of Theorem 6

We first show that problem (29) can be equivalently transformed into problem (34). We introduce a set of new non-negative variables:

$$\hat{p}_j=t_jp_j,\hat{q}_i=t_{M+i}q_i,\quad \forall i\in\mathcal{N},j\in\mathcal{J}_i. \quad \text{(F.1)}$$

Substituting (F.1) into problem (29), we show that problem (29) is equivalent to problem (34).

Then, we show that problem (34) is a convex problem. Since constraints (34e)-(34i) are all linear, we only need to check that objective function (34a) and constraints (34b)-(34d) are convex. Due to the fact that $-\bar{u}(|h_{nj}|^2\hat{q}_n)$ is convex w.r.t. $\hat{q}_n$ from (D.3), $-t_{M+n}\bar{u}\left(\frac{|h_{nj}|^2\hat{q}_n}{t_{M+n}}\right)$ is convex w.r.t. $(t_{M+n},\hat{q}_n)$ according to the property of perspective function [57, Page 89]. Thus, objective function (34a) is convex. Analogously, constraints (34b)-(34d) can also be shown convex. As a result, problem (34) is a convex problem.

References

[1] Z. Yang, Y. Pan, W. Xu, R. Guan, Y. Wang, and M. Chen, "Energy efficient resource allocation for machine-to-machine communications with NOMA and energy harvesting," in *Proc. IEEE Int. Conf. Compt. Commun. Workshops*, Atlanta, GA, USA, May 2017, pp. 1–6.

[2] G. Wu, S. Talwar, K. Johnsson, and N. Himayat, "M2M: From mobile to embedded internet," *IEEE Commun. Mag.*, vol. 49, no. 4, pp. 36–43, Apr. 2011.

[3] K. Zheng, F. Hu, W. Wang, and W. Xiang, "Radio resource allocation in LTE-advanced cellular networks with M2M communications," *IEEE Commun. Mag.*, vol. 50, no. 7, pp. 184–192, Jul. 2012.

[4] M. Hasan, E. Hossain, and D. Niyato, "Random access for machine-to-machine communication in LTE-advanced networks: Issues and approaches," *IEEE Commun. Mag.*, vol. 51, no. 6, pp. 86–93, Jun. 2013.

[5] K. Zheng, S. Ou, J. Alonso-Zarate, M. Dohler, F. Liu, and H. Zhu, "Challenges of massive access in highly dense LTE-advanced networks with machine-to-machine communications," *IEEE Wireless Commun.*, vol. 21, no. 3, pp. 12–18, Jun. 2014.

[6] D. Niyato, P. Wang, and D. I. Kim, "Performance modeling and analysis of heterogeneous machine type communications," *IEEE Trans. Wireless Commun.*, vol. 13, no. 5, pp. 2836–2849, May 2014.

[7] M. Condoluci, M. Dohler, G. Araniti, A. Molinaro, and K. Zheng, "Toward 5G densenets: Architectural advances for effective machine-type communications over femtocells," *IEEE Commun. Mag.*, vol. 53, no. 1, pp. 134–141, Jan. 2015.

[8] A. Aijaz, M. Tshangini, M. R. Nakhai, X. Chu, and A. H. Aghvami, "Energy-efficient uplink resource allocation in LTE networks with M2M/H2H co-existence under statistical QoS guarantees," *IEEE Trans. Commun.*, vol. 62, no. 7, pp. 2353–2365, Jul. 2014.

[9] G. Zhang, A. Li, K. Yang, L. Zhao, and D. Cheng, "Optimal power control for delay-constraint machine type communications over cellular uplinks," *IEEE Commun. Lett.*, vol. 20, no. 6, pp. 1168–1171, Jun. 2016.

[10] G. Zhang, A. Li, K. Yang, L. Zhao, Y. Du, and D. Cheng, "Energy-efficient power and time-slot allocation for cellular-enabled machine type communications," *IEEE Commun. Lett.*, vol. 20, no. 2, pp. 368–371, Feb. 2016.

[11] Y. Saito, Y. Kishiyama, A. Benjebbour, T. Nakamura, A. Li, and K. Higuchi, "Non-orthogonal multiple access (NOMA) for cellular future radio access," in *Proc. IEEE Veh. Technol. Conf.*, Dresden, German, Jun. 2013, pp. 1–5.

[12] Z. Yang, C. Pan, W. Xu, Y. Pan, M. Chen, and M. Elkashlan, "Power control for multi-cell networks with non-orthogonal multiple access," *IEEE Trans. Wireless Commun.*, vol. PP, no. 99, pp. 1–1, 2017.

[13] Z. Ding, Y. Liu, J. Choi, Q. Sun, M. Elkashlan, and H. V. Poor, "Application of non-orthogonal multiple access in LTE and 5G networks," *IEEE Commun. Mag.*, vol. 55, no. 2, pp. 185–191, Feb. 2017.

[14] X. Chen, A. Benjebbour, A. Li, and A. Harada, "Multi-user proportional fair scheduling for uplink non-orthogonal multiple access (NOMA)," in *Proc. IEEE Veh. Technol. Conf.*, Seoul, Korea, May 2014, pp. 1–5.

[15] M. Al-Imari, P. Xiao, M. A. Imran, and R. Tafazolli, "Uplink non-orthogonal multiple access for 5G wireless networks," in *Proc. IEEE Int. Symp. Wireless Commun. Syst.*, Barcelona, Spain, Aug. 2014, pp. 781–785.

[16] N. Zhang, J. Wang, G. Kang, and Y. Liu, "Uplink nonorthogonal multiple access in 5G systems," *IEEE Commun. Lett.*, vol. 20, no. 3, pp. 458–461, Mar. 2016.

[17] Z. Yang, W. Xu, H. Xu, J. Shi, and M. Chen, "Energy efficient non-orthogonal multiple access for machine-to-machine communications," *IEEE Commun. Lett.*, vol. 21, no. 4, pp. 817–820, Apr. 2017.

[18] D. Malak, H. S. Dhillon, and J. G. Andrews, "Optimizing data aggregation for uplink machine-to-machine communication networks," *IEEE Trans. Commun.*, vol. 64, no. 3, pp. 1274–1290, Mar. 2016.

[19] H. S. Dhillon, H. C. Huang, H. Viswanathan, and R. A. Valenzuela, "Power-efficient system design for cellular-based machine-to-machine communications," *IEEE Trans. Wireless Commun.*, vol. 12, no. 11, pp. 5740–5753, Nov. 2013.

[20] X. Xiong, K. Zheng, R. Xu, W. Xiang, and P. Chatzimisios, "Low power wide area machine-to-machine networks: Key techniques and prototype," *IEEE Commun. Mag.*, vol. 53, no. 9, pp. 64–71, Sep. 2015.

[21] L. R. Varshney, "Transporting information and energy simultaneously," in *Proc. IEEE Int. Symp. Inf. Theory*, Toronto, ON, Canada, Jul. 2008, pp. 1612–1616.

[22] S. Bi, C. K. Ho, and R. Zhang, "Wireless powered communication: Opportunities and challenges," *IEEE Commun. Mag.*, vol. 53, no. 4, pp. 117–125, Apr. 2015.

[23] X. Huang and N. Ansari, "Energy sharing within EH-enabled wireless communication networks," *IEEE Wireless Commun.*, vol. 22, no. 3, pp. 144–149, Jun. 2015.

[24] X. Huang, T. Han, and N. Ansari, "On green-energy-powered cognitive radio networks," *IEEE Commun. Surveys Tut.*, vol. 17, no. 2, pp. 827–842, Secondquarter 2015.

[25] T. K. Thuc, E. Hossain, and H. Tabassum, "Downlink power control in two-tier cellular networks with energy-harvesting small cells as stochastic games," *IEEE Trans. Commun.*, vol. 63, no. 12, pp. 5267–5282, Dec. 2015.

[26] S. Lohani, E. Hossain, and V. K. Bhargava, "On downlink resource allocation for SWIPT in small cells in a two-tier HetNet," *IEEE Trans. Wireless Commun.*, vol. 15, no. 11, pp. 7709–7724, Nov. 2016.

[27] S. Maghsudi and E. Hossain, "Distributed user association in energy harvesting small cell networks: An exchange economy with uncertainty," *IEEE Trans. Green Commun. Netw.*, vol. 1, no. 3, pp. 294–308, Sep. 2017.

[28] D. W. K. Ng and R. Schober, "Energy-efficient power allocation for M2M communications with energy harvesting transmitter," in *Proc. IEEE Global Commun. Conf. Workshops*, Anaheim, CA, USA, Dec. 2012, pp. 1644–1649.

[29] J. Rinne, J. Keskinen, P. R. Berger, D. Lupo, and M. Valkama, "Viability bounds of M2M communication using energy-harvesting and passive wake-up radio," *IEEE Access*, vol. PP, no. 99, pp. 1–1, 2017.

[30] M. A. Andersson, A. Özçelikkale, M. Johansson, U. Engström, A. Vorobiev, and J. Stake, "Feasibility of ambient RF energy harvesting for self-sustainable M2M communications using transparent and flexible graphene antennas," *IEEE Access*, vol. 4, pp. 5850–5857, 2016.

[31] Z. Yang, W. Xu, Y. Pan, R. Guan, and M. Chen, "Energy minimization in machine-to-machine systems with energy harvesting," in *Proc. IEEE Veh. Technol. Conf.*, Sydney, Austrlia, Jun. 2017, pp. 1–5.

[32] A. A. Nasir, X. Zhou, S. Durrani, and R. A. Kennedy, "Relaying protocols for wireless energy harvesting and information processing," *IEEE Trans. Wireless Commun.*, vol. 12, no. 7, pp. 3622–3636, Jul. 2013.

[33] Y. Liu, S. A. Mousavifar, Y. Deng, C. Leung, and M. Elkashlan, "Wireless energy harvesting in a cognitive relay network," *IEEE Trans. Wireless Commun.*, vol. 15, no. 4, pp. 2498–2508, Apr. 2016.

[34] S. Atapattu and J. Evans, "Optimal energy harvesting protocols for wireless relay networks," *IEEE Trans. Wireless Commun.*, vol. 15, no. 8, pp. 5789–5803, Aug. 2016.

[35] X. Huang and N. Ansari, "Optimal cooperative power allocation for energy-harvesting-enabled relay networks," *IEEE Trans. Veh. Technol.*, vol. 65, no. 4, pp. 2424–2434, Apr. 2016.

[36] H. Kim and G. de Veciana, "Leveraging dynamic spare capacity in wireless systems to conserve mobile terminals' energy," *IEEE/ACM Trans. Netw.*, vol. 18, no. 3, pp. 802–815, Jun. 2010.

[37] V. Angelakis, A. Ephremides, Q. He, and D. Yuan, "Minimum-time link scheduling for emptying wireless systems: Solution characterization and algorithmic framework," *IEEE Trans. Inf. Theory*, vol. 60, no. 2, pp. 1083–1100, Feb. 2014.

[38] C. K. Ho, D. Yuan, L. Lei, and S. Sun, "Power and load coupling in cellular networks for energy optimization," *IEEE Trans. Wireless Commun.*, vol. 14, no. 1, pp. 509–519, Jan. 2015.

[39] S. Karmakar and M. K. Varanasi, "The diversity-multiplexing tradeoff of the dynamic decode-and-forward protocol on a MIMO half-duplex relay channel," *IEEE Trans. Inf. Theory*, vol. 57, no. 10, pp. 6569–6590, Oct. 2011.

[40] S.-E. Wei, H.-Y. Hsieh, and H.-J. Su, "Joint optimization of cluster formation and power control for interference-limited machine-to-machine communications," in *IEEE Global Commun. Conf.*, Anaheim, CA, USA, Dec. 2012, pp. 5512–5518.

[41] T.-C. Juan, S. E. Wei, and H. Y. Hsieh, "Data-centric clustering for data gathering in machine-to-machine wireless networks," in *IEEE Int. Conf. Commun. Workshops*, Budapest, Hungary, Jun. 2013, pp. 89–94.

[42] G. Miao, A. Azari, and T. Hwang, "E^2-MAC: Energy efficient medium access for massive m2m communications," *IEEE Trans. Commun.*, vol. 64, no. 11, pp. 4720–4735, Nov. 2016.

[43] H. Tabassum, E. Hossain, and J. Hossain, "Modeling and analysis of uplink non-orthogonal multiple access in large-scale cellular networks using poisson cluster processes," *IEEE Trans. Commun.*, vol. 65, no. 8, pp. 3555–3570, Aug. 2017.

[44] A. Zafar, M. Shaqfeh, M. S. Alouini, and H. Alnuweiri, "On multiple users scheduling using superposition coding over rayleigh fading channels," *IEEE Commun. Lett.*, vol. 17, no. 4, pp. 733–736, Apr. 2013.

[45] M. A. Sedaghat and R. R. Müller, "On user pairing in NOMA uplink," *CoRR*, vol. abs/1707.01846, 2017. [Online]. Available: http://arxiv.org/abs/1707.01846

[46] Z. Ding, P. Fan, and H. V. Poor, "Impact of user pairing on 5G nonorthogonal multiple-access downlink transmissions," *IEEE Trans. Veh. Technol.*, vol. 65, no. 8, pp. 6010–6023, Aug. 2016.

[47] M. Shirvanimoghaddam, M. Condoluci, M. Dohler, and S. J. Johnson, "On the fundamental limits of random non-orthogonal multiple access in cellular massive iot," *IEEE J. Sel. Areas Commun.*, vol. 35, no. 10, pp. 2238–2252, Oct. 2017.

[48] H. Ju and R. Zhang, "Throughput maximization in wireless powered communication networks," *IEEE Trans. Wireless Commun.*, vol. 13, no. 1, pp. 418–428, Jan. 2014.

[49] ——, "Optimal resource allocation in full-duplex wireless-powered communication network," *IEEE Trans. Commun.*, vol. 62, no. 10, pp. 3528–3540, Oct. 2014.

[50] X. Zhou, R. Zhang, and C. K. Ho, "Wireless information and power transfer in multiuser OFDM systems," *IEEE Trans. Wireless Commun.*, vol. 13, no. 4, pp. 2282–2294, Dec. 2014.

[51] M. Guillaud, D. T. Slock, and R. Knopp, "A practical method for wireless channel reciprocity exploitation through relative calibration." in *Proc. Int. Symp. Signal Process. Its Applcat.*, Sydney, Australia, Aug. 2005, pp. 403–406.

[52] E. Boshkovska, D. W. K. Ng, N. Zlatanov, and R. Schober, "Practical non-linear energy harvesting model and resource allocation for SWIPT systems," *IEEE Commun. Lett.*, vol. 19, no. 12, pp. 2082–2085, Dec. 2015.

[53] E. Boshkovska, R. Morsi, D. W. K. Ng, and R. Schober, "Power allocation and scheduling for SWIPT systems with non-linear energy harvesting model," in *IEEE Int. Conf. Commun.*, May 2016, pp. 1–6.

[54] Q. Wu, W. Chen, M. Tao, J. Li, H. Tang, and J. Wu, "Resource allocation for joint transmitter and receiver energy efficiency maximization in downlink OFDMA systems," *IEEE Trans. Commun.*, vol. 63, no. 2, pp. 416–430, Feb. 2015.

[55] Q. Wu, M. Tao, D. W. K. Ng, W. Chen, and R. Schober, "Energy-efficient resource allocation for wireless powered communication networks," *IEEE Trans. Wireless Commun.*, vol. 15, no. 3, pp. 2312–2327, Mar. 2016.

[56] D. W. K. Ng, E. S. Lo, and R. Schober, "Wireless information and power transfer: Energy efficiency optimization in OFDMA systems," *IEEE Trans. Wireless Commun.*, vol. 12, no. 12, pp. 6352–6370, Dec. 2013.

[57] S. Boyd and L. Vandenberghe, *Convex Optimization*. Cambridge University Press, 2004.

[58] *Evolved Universal Terrestrial Radio Access (E-UTRA); Further advancements for E-UTRA physical layer aspects*, 3GPP TR 36.814 V9. 0.0, Mar. 2010.

[59] J. Guo and X. Zhu, "An improved analytical model for rf-dc conversion efficiency in microwave rectifiers," in *IEEE/MTT-S Int. Microwave Symp. Digest*, Montreal, QC, Canada, Jun. 2012, pp. 1–3.